

Hydrodynamic stability of multi-layer Hele-Shaw flows

Prabir Daripa

Department of Mathematics, Texas A&M University, College Station,
TX 77843, USA

E-mail: prabir.daripa@math.tamu.edu

Received 29 September 2008

Accepted 19 November 2008

Published 10 December 2008

Online at stacks.iop.org/JSTAT/2008/P12005

doi:10.1088/1742-5468/2008/12/P12005

Abstract. Upper bound results on the growth rate of unstable multi-layer Hele-Shaw flows are obtained in this paper. The cases treated are constant viscosity layers and variable viscosity layers. As an application of the bound, we obtain some sufficient conditions for suppressing instability of two-layer flows by introducing an arbitrary number of constant viscosity fluid layers in between. This sufficient condition has very practical relevance because it narrows the choice of internal-layer fluids on the basis of the surface tensions of all interfaces and viscosities of fluids in various layers. The importance of this condition which has been hitherto unknown is also discussed. Other consequences of these upper bounds and sufficient conditions are discussed. The case of internal fluid layers having stable and unstable viscous profiles is also treated for three-layer and four-layer flows. The connection of these variable viscosity results to viscous fingering in complex fluids is also established. Implications of these stability results for these various multi-layer flows are discussed and compared from a practical standpoint.

Keywords: hydrodynamic instabilities, hydrodynamic waves, flow in porous media

Contents

1. Introduction	2
2. Background	5
3. Three-layer flows	9
3.1. A classic result on the upper bound	9
3.2. A useful lemma	11
3.3. Some notation	12
3.4. New improved results on the upper bound	13
3.5. Best estimates on modal and absolute upper bounds	14
3.6. Stability enhancement	16
3.6.1. Role of long waves.	16
3.6.2. Role of short waves.	17
3.6.3. Sufficient conditions for stability enhancement.	18
4. Four-layer flows	19
4.1. Upper bounds based on asymptotics	22
4.2. Sufficient conditions for stability enhancement	23
5. Multi-layer flows	23
5.1. Sufficient conditions for stability enhancement	24
5.2. Upper bounds based on asymptotics	25
5.3. Determination of the number of layers from the prescribed arbitrary growth rate of instability	25
6. Three-layer flows	26
7. Four-layer flows	28
8. Conclusions	30
Acknowledgment	31
References	31

1. Introduction

Interfacial flows are ubiquitous in Nature and play very important roles in many areas of science and technology. Over the last few decades, there have been significant advances in the theory and modeling of flows involving only one interface. However, research on flows involving more than one interface, though ongoing, is still very primitive. Quantitatively useful theory and efficient accurate modeling techniques for such multi-interface flows are few in comparison, though interaction of interfaces with each other and with the incompressible fluid around these can be explained easily in a qualitative sense using laws of physics. We take the fluid to be incompressible for ease of explanation. Since the fluid between any two interfaces is incompressible, the amount of fluid between two interfaces cannot change due to conservation of mass. Therefore, in general an arbitrary motion of

one interface, however small, must induce motion of the other interface; otherwise it will violate the principle of conservation of mass. The only way it can do this is to cause fluid flow in between the interfaces. This basic mechanism in multi-layer flows explains that an infinitesimal disturbance of even one interface will cause fluid flows and motion of all other interfaces, however small. Similarly, using conservation laws one can understand the mechanism behind stabilization or destabilization of any specific interface. We provide a simplistic explanation: for destabilization of an interface, energy of the fluid surrounding this interface will feed into its motion and vice versa for stabilization.

Mathematical equations governing the evolution of interfacial disturbances are well understood and it is accessible to mathematical analysis within linear theory in the single-interface case for many flows. This allows reliable prediction of the effect of various fluids and interfacial properties on the growth of interfacial disturbances. In turn, this knowledge also guides selection of correct fluid and interfacial properties *a priori* to achieve desirable enhancement or suppression of instability of interfacial flows. In contrast, the mathematical theory of stability of multi-interface flows is much less well developed. Understanding of similar issues even for two-interface, or equivalently three-layer, flows is incomplete. The prediction and the selection problems, similar to the ones discussed above for the single-interface case, are open problems for most multi-interface flows. Such problems are commonly solved from extrapolation of single-interface results due to lack of useful theoretical results for such multi-interface flows. This aspect of multi-interface flow problems is further discussed below using viscosity driven instability in Newtonian incompressible fluids.

The displacement of a more viscous fluid by a less viscous one is known to be potentially unstable in a Hele-Shaw cell. Such flows first studied by Hele-Shaw [1] are known as Hele-Shaw flows and have similarities with flows through porous media [2] in the sense that in both of these flows, fluid velocity is proportional to the pressure gradient. Because of this analogy and relative ease and accuracy with which such Hele-Shaw flows can be experimentally studied in comparison to flows in porous media, Hele-Shaw flows have been studied extensively over many decades. The instability theory in this context, also known as Saffman–Taylor instability [3], is now well developed for single-interface flows. Exact growth rates of interfacial disturbances for such flows are well known and well documented in standard textbooks on hydrodynamic stability theory, e.g. Drazin and Reid [4]. For our introduction below and later reference in this paper, it is worth citing some exact results for rectilinear flows. If μ_r is the viscosity of the displaced fluid, μ_l ($\mu_l < \mu_r$) is the viscosity of the displacing fluid, U is the constant velocity of the rectilinear flow, and the surface tension at the interface is T , then the growth rate σ_{st} of the interfacial disturbance having wavenumber k is given by

$$\sigma_{st}(k) = \frac{Uk(\mu_r - \mu_l) - k^3T}{\mu_r + \mu_l}, \quad (1)$$

from which it follows that the growth rate of any unstable wave cannot exceed σ_{st}^u :

$$\sigma_{st} \leq \sigma_{st}^u = \frac{2T}{(\mu_r + \mu_l)} \left(\frac{U(\mu_r - \mu_l)}{3T} \right)^{3/2}. \quad (2)$$

These formulae imply that increasing the interfacial surface tension suppresses instability whereas increasing the positive viscosity jump at the interface in the direction of flow

further enforces instability [4]. On the basis of this understanding, it is common practice to use a layer of third fluid in between having viscosity less than that of the displaced fluid and more than that of the displacing fluid, in the hope that it will suppress the growth of instability that is otherwise present in the absence of this middle layer [5]–[7]. This expectation is justified on the basis of the application of our understanding of single-interface flows to multi-interface case under the assumptions that (i) there is minimal or favorable interfacial interaction and (ii) surface tensions at two interfaces are similar to the surface tension at the original interface between the displaced and the displacing fluid in the absence of the middle layer. This makes each of these interfaces less unstable individually due to reduction in the viscosity jump across them. However, when surface tensions as well as the viscosity jumps at two interfaces are significantly modified due to the middle-layer fluid, it is not easy to correctly predict the outcome of these collective effects on the overall instability of these flows from simple extrapolation of our understanding of single-interface flows. This problem becomes even more daunting in the case of flows with arbitrary number of interfaces. This paper makes a theoretical attempt to partially address these issues by extending and building on our previous work on the upper bound on growth rates of disturbances in three-layer flows.

For the three-layer case, an absolute upper bound of the growth rate, using Gerschgorin’s localization theorem on a discrete version of the continuous flow problem, has been derived earlier in [8]. A simpler derivation of the same bound using a weak formulation has been derived recently in [9]. The absolute upper bound reported there is in non-strict inequality form meaning, in practice, that this bound will not be reached for a non-trivial disturbance as discussed in [10]. In [10], it was shown how this bound reduces to a strict inequality for a non-trivial disturbance and how to improve upon it by taking physics into consideration. Several interesting theoretical results were reported there that are independent of the length of the middle layer as well as a numerical study of the interfacial instability transfer mechanism being presented.

In this paper, we further build on these works in several respects. In particular, in Part I we consider interfacial flows which have arbitrary number of individually unstable interfaces (meaning that the viscosity jump is positive in the direction of flow at each of the interfaces) but individually stable constant viscosity layers. In Part II, we have partially extended the results of Part I when layers themselves are also individually unstable. This case is significantly more difficult as we will see later. To be specific:

- (1) In section 2, the problem is formulated mathematically.
- (2) In section 3.1, the stability problem (see section 5 of [8]) for three-layer flows with constant viscosity layers is revisited and the old classic result on the upper bound on the growth rate is presented. To improve upon this bound, a new inequality involving an integral is derived in section 3.2. Then using this new inequality, continuous families of upper bound estimates (see inequality (45)) indexed by two parameters are obtained in section 3.4. By sweeping over the range of values that these parameters can take, an estimate (see (47)) of the modal upper bound σ_1^m (the subscript ‘1’ above refers to one internal layer or equivalently a three-layer case) is obtained. From this, an absolute upper bound σ_1^u (see (49)) on the growth rate of a non-trivial disturbance is obtained in a non-strict form without taking into account any ad hoc physical considerations. This new bound is shown to be an improvement over the upper

bounds known to date. An explicit and useful good approximation (see (53)) to this absolute upper bound is also derived here. In section 3.6, roles of short and long waves are first investigated. Then in section 3.6.3, as an application of this new absolute upper bound, we obtain an exact theoretical result embodying collective competing effects of interfacial viscosity jumps and surface tension forces. This result provides a family of sufficient conditions for suppression of instability which is useful in the selection of middle-layer fluid based on its interfacial surface tension properties with the extreme-layer fluids and their viscosities. Strikingly, this family includes a sufficient condition that does not depend on the viscosity of the middle-layer fluid.

- (3) In section 4, we extend the above results first to four-layer flows which are more amenable to and provide an inductive basis for generalization to flows involving arbitrary number of unstable interfaces separated by constant viscosity layers.
- (4) In section 5, using results of section 4 as an inductive basis we generalize results of section 3 to flows with arbitrary number of constant viscosity layers. In addition, in section 5.3 as another application of our results we prescribe a solution to the following inverse problem: determine the number of layers of constant viscosity fluid from the prescribed maximal growth rate of the instability.
- (5) In section 6, we briefly revisit the stability problem [9] for three-layer flows with unstable viscosity profile in the middle layer. Extending results from flows with constant viscosity layers to flows with two or more individually unstable internal layers is difficult, which has been discussed in section 7. In section 7 where four-layer flows with internal layers having unstable viscosity profiles are treated, we are able to obtain some results on the upper bound and some interesting consequences of these results. This section makes it clear that the tools of analysis that are used in this paper are not sufficient to provide any interesting results on an upper bound for flows with arbitrary number of individually unstable internal fluid layers beyond 1.
- (6) Finally we conclude and provide a summary of this work in section 8.

In closing this section, it is important to emphasize that though this work was originally motivated by enhancing oil recovery from porous media, the paper mainly deals with stability of multi-layer Hele-Shaw flows and provides many new stability results of fundamental interest. In fact, there are no theoretical results on multi-layer Hele-Shaw flows and this paper is the first of its kind. Moreover, the technique applied in the paper is of general interest and may be applicable to other multi-layer flows such as multi-layer Rayleigh–Taylor instabilities.

2. Background

We first review the physical set-up of the problem and its mathematical formulation [11].

The physical set-up consists of two-dimensional fluid flows in a three-layer Hele-Shaw cell as shown in figure 1. The domain Ω of interest is then $\Omega := (x, y) = \mathbb{R}^2$ (with a periodic extension of the set-up in the y direction). The fluid upstream (i.e., as $x \rightarrow -\infty$) has a velocity $\mathbf{u} = (U, 0)$. The fluid in the left layer with constant viscosity μ_1 extends up

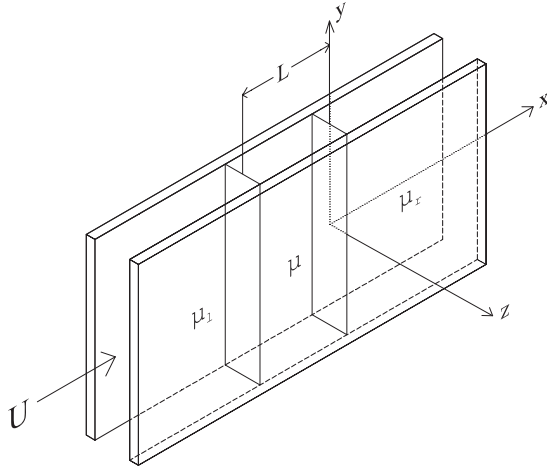


Figure 1. Three-layer fluid flow in a Hele-Shaw cell.

to $x = -\infty$, the fluid in the right layer with constant viscosity μ_r extends up to $x = \infty$, and the fluid in between middle layer of length L has a smooth viscous profile $\mu(x)$ with $\mu_1 < \mu(x) < \mu_r$. The underlying equations of this problem are

$$\nabla \cdot \mathbf{u} = 0, \quad \nabla p = -\mu \mathbf{u}, \quad \frac{\partial \mu}{\partial t} + \mathbf{u} \cdot \nabla \mu = 0, \quad (3)$$

where $\nabla = (\frac{\partial}{\partial x}, \frac{\partial}{\partial y})$. The first equation (3)₁ is the continuity equation for incompressible flow, the second equation (3)₂ is the Darcy law [2], and the third equation (3)₃ is the advection equation for viscosity [11, 12]. Equation (3)₂ has been used successfully in modeling Hele-Shaw flows for a long time [1]. For example, Taylor showed in physical experiments development of fingers in a Hele-Shaw cell which were also obtained analytically by Saffman and Taylor [3] using the Darcy law (3)₂ for modeling velocity. There is a rich history to this in fluid mechanics [13, 14]. The advection equation (3)₃ for viscosity arises from the continuity equation of species such as polymer in water which is simply being advected and viscosity of this poly-solution (polymer in water) is an invertible function of the polymer concentration. More details of this can be found in [11].

The above system admits a simple basic solution: the whole fluid set-up moves with speed U in the x direction and the two interfaces, namely the one separating the left layer from the middle layer and the other separating the right layer from the middle layer, are planar (i.e. parallel to the y - z plane). The pressure corresponding to this basic solution is obtained by integrating (3)₂. In a frame moving with velocity $(U, 0)$, the above system is stationary along with two planar interfaces separating these three fluid layers. Here and below, with slight abuse of notation, the same variable x is used in the moving reference frame.

In the moving frame, the basic solution $(u = 0, v = 0, p_0(x), \mu(x))$ is perturbed by $(\epsilon \tilde{u}, \epsilon \tilde{v}, \epsilon \tilde{p}, \epsilon \tilde{\mu})$, where ϵ is a small parameter. We write equations (3)₁–(3)₃ in the above moving frame and then substitute the perturbed variables in these modified equations. We equate to zero the coefficients of the small parameter ϵ to obtain the following linearized

equations for $\tilde{\mathbf{u}} = (\tilde{u}, \tilde{v})$, \tilde{p} , and $\tilde{\mu}$:

$$\nabla \cdot \tilde{\mathbf{u}} = 0, \quad (4)$$

$$\nabla \tilde{p} = -\mu \tilde{\mathbf{u}} - \tilde{\mu} (U, 0), \quad (5)$$

$$\frac{\partial \tilde{\mu}}{\partial t} + \tilde{u} \frac{d\mu}{dx} = 0. \quad (6)$$

We study temporal evolution of arbitrary perturbations by the method of normal modes. Hence, we consider typical wave components of the form

$$(\tilde{u}, \tilde{v}, \tilde{p}, \tilde{\mu}) = (f(x), \tau(x), \psi(x), \phi(x)) e^{(iky + \sigma t)}, \quad (7)$$

where k is a real axial wavenumber, and σ is the growth rate which could be complex. The ansatz (7) is consistent with (4)–(6) provided

$$\tau(x) = ik^{-1}f_x, \quad \psi(x) = -k^{-2}\mu(x)f_x, \quad \phi(x) = -\sigma^{-1}f(x)\mu_x, \quad (8)$$

where f_x denotes the derivative function of $f(x)$. In general, functions $f(x)$, $\tau(x)$, $\psi(x)$, and $\phi(x)$ could be complex since the disturbances $\tilde{u}, \tilde{v}, \tilde{p}, \tilde{\mu}$ in the ansatz (7) are real. However, it has been shown in [9] that these are real including the growth rate σ . Therefore, these variables will be treated as real for our purposes below.

Cross differentiating the x and y components of the vector pressure equation (5) and using the ansatz (7) and (8), we obtain

$$\mu(f_{xx} - k^2 f) + \mu_x f_x + \frac{k^2 U}{\sigma} \mu_x f = 0, \quad x \neq -L, 0. \quad (9)$$

Note that coefficients of this equation depend on k only in its even power (2 to be specific). Therefore, without any loss of generality, below we take $k \geq 0$ which is equivalent to writing $|k|$ for k below, which is consistent with the above equation. Recall that $\mu(x) = \mu_l, x < -L$ and $\mu_x = \mu_r > \mu_l, x > 0$. Therefore, in the two extreme layers this equation simplifies to

$$f_{xx} - k^2 f = 0, \quad x < -L, \quad x > 0. \quad (10)$$

The far-field boundary conditions $f \rightarrow 0$ as $x \rightarrow \mp\infty$ then give the following solutions in the exterior of middle layer:

$$\begin{aligned} f(x) &= f(-L) \exp(k(x+L)), & \text{for } x < -L, \\ f(x) &= f(0) \exp(-kx), & \text{for } x > 0. \end{aligned} \quad (11)$$

We know that the basic state has two planar interfaces at $x = 0$ and $-L$ in the moving frame. For general treatment of the derivation of the boundary conditions at these interfaces, let a planar undisturbed interface be located at $x = x_0$. If this planar surface is disturbed slightly such that its equation becomes $x = x_0 + \tilde{\eta}(y, t)$, then the kinematic condition that each particle remains there gives

$$\tilde{\eta}_t = \tilde{u}(x, y, t) \approx \tilde{u}(x_0, y, t), \quad \text{on } x = x_0 + \tilde{\eta}(y, t), \quad (12)$$

and the last approximation in the above equation uses linear approximation assuming that the perturbation is small. It then follows from (7)₁ and (12) that

$$\tilde{\eta}(y, t) = (f(x_0)/\sigma) \exp(iky + \sigma t). \quad (13)$$

Thus kinematic boundary condition at the interface provides the equation of the interface in terms of function $f(x)$. This is used below to obtain relevant equations from the dynamic boundary condition for the interface. This condition, within linear approximation, is given by

$$p^+(x) - p^-(x) = T\tilde{\eta}_{yy}(x), \quad \text{on } x = x_0 + \tilde{\eta}(y, t), \quad (14)$$

where the superscripts '+' and '-' are used to denote the 'right' and 'left' limit values (direction from 'left' to 'right' is in the positive direction of the x axis), T is the surface tension and $\tilde{\eta}_{yy}$ is the approximate curvature of the perturbed interface. Above and below, h_y denotes the derivative of an arbitrary function $h(y)$ with respect to y .

The pressure at the perturbed interfaces will be discontinuous due to curvature effects and associated surface tension force. We have the following expression for the pressure at the interface $x = x_0 + \tilde{\eta}(y, t)$ as we approach it from the right:

$$\begin{aligned} p^+(x_0 + \tilde{\eta}(y, t)) &= p_0^+(x_0 + \tilde{\eta}(y, t)) + \tilde{p}^+(x_0 + \tilde{\eta}(y, t)) \\ &\approx p_0(x_0) + \tilde{\eta}(y, t) \cdot (\partial p_0^+ / \partial x)|_{x=x_0} + \tilde{p}^+(x_0), \end{aligned} \quad (15)$$

where the approximation above retains only the linear term in perturbation. The basic pressure $p_0(x_0)$ is continuous across the planar interface profile of the basic state. The right limit values $(\partial p_0^+ / \partial x)|_{x=x_0}$ from (6) and $\tilde{p}^+(x_0)$ from (7) and (8) are given by

$$\partial p_0^+ / \partial x(x_0) = -U\mu^+(x_0), \quad \tilde{p}^+(x_0) = -(\mu^+(x_0) f_x^+(x_0) / k^2) \exp(iky + \sigma t), \quad (16)$$

and similar expressions can be obtained for corresponding left limit values. Substituting (16) into (15) provides the right limit value of the pressure at the perturbed interface $x = x_0 + \tilde{\eta}(y, t)$ and similar expressions and manipulations provide the left limit value of the pressure at the interface. These are

$$p^+(x_0 + \tilde{\eta}(y, t)) = p_0(x_0) - \mu^+(x_0) \left\{ \frac{f_x^+(x_0)}{k^2} + \frac{U}{\sigma} f(x_0) \right\} \exp(iky + \sigma t), \quad (17)$$

$$p^-(x_0 + \tilde{\eta}(y, t)) = p_0(x_0) - \mu^-(x_0) \left\{ \frac{f_x^-(x_0)}{k^2} + \frac{U}{\sigma} f(x_0) \right\} \exp(iky + \sigma t). \quad (18)$$

Using (17) and (18) in the linearized dynamic condition (14) gives

$$\mu^-(x_0) \left\{ \frac{f_x^-(x_0)}{k^2} + \frac{U}{\sigma} f(x_0) \right\} - \mu^+(x_0) \left\{ \frac{f_x^+(x_0)}{k^2} + \frac{U}{\sigma} f(x_0) \right\} = -T \frac{k^2 f(x_0)}{\sigma}, \quad (19)$$

or equivalently

$$(\mu^- f_x^- f)(x_0) - (\mu^+ f_x^+ f)(x_0) = \frac{k^2 U [\mu^+(x_0) - \mu^-(x_0)] - k^4 T}{\sigma} f^2(x_0). \quad (20)$$

This equation holds at each of the two interfaces, one at $x_0 = 0$ with surface tension T_0 and the other at $x = -L$ with surface tension T_1 . In this equation for the interface at $x_0 = -L$, we use $f_x^-(-L) = kf(-L)$ from (11), and similarly for the interface at $x_0 = 0$, we use $f_x^+(0) = -kf(0)$ from (11). Therefore, from equation (20) for these two interfaces we obtain

$$\begin{aligned} -(\mu^- f_x^- f)(0) &= \mu_r k f^2(0) - \frac{E_0}{\sigma} f^2(0), \\ (\mu^+ f_x^+ f)(-L) &= \mu_l k f^2(-L) - \frac{E_1}{\sigma} f^2(-L), \end{aligned} \quad (21)$$

where

$$E_0 = k^2 U[\mu_r - \mu^-(0)] - T_0 k^4, \quad E_1 = k^2 U[\mu^+(-L) - \mu_1] - T_1 k^4. \quad (22)$$

The mathematical problem for this three-layer case is defined by the field equation (9), far-field boundary conditions (11) and two interfacial conditions (21).

In Part I below, we first consider the above problem with constant viscosity fluid in the middle layer and obtain results which go beyond our previously reported results in [15] on this problem. Then we generalize these results to a multi-layer case with arbitrary number of interfaces separating constant viscosity fluids. In Part II, we provide results on upper bounds and their consequences for three-layer and four-layer flows with variable viscous profiles for the internal layers. Difficulties for extending these results to a multi-layer case are addressed in this part.

Part I: Constant viscosity fluid layers

3. Three-layer flows

3.1. A classic result on the upper bound

Consider that the fluid in the intermediate layer has constant viscosity μ_1 with $\mu_l < \mu_1 < \mu_r$. Then the problem for the middle region $[-L, 0]$ defined by equation (9) and the two interfacial conditions (21) reduces to

$$\begin{aligned} f_{xx} - k^2 f &= 0, \\ -\mu_1 (f_x^- f)(0) &= (\mu_r k - \sigma^{-1} E_0) f^2(0), \\ \mu_1 (f_x^+ f)(-L) &= (\mu_l k - \sigma^{-1} E_1) f^2(-L), \end{aligned} \quad (23)$$

where

$$E_0 = \{[\mu]_r U k^2 - T_0 k^4\}, \quad E_1 = \{[\mu]_l U k^2 - T_1 k^4\}. \quad (24)$$

Above and below, we have used the notation $[\mu]_l = (\mu_1 - \mu_l)$ and $[\mu]_r = (\mu_r - \mu_1)$. Multiplying (23)₁ with $f(x)$ and then integrating on the interval $(-L, 0)$ leads to

$$(f_x^+ f)(-L) - (f_x^- f)(0) + \int_{-L}^0 f_x^2 dx + k^2 \int_{-L}^0 f^2 dx = 0, \quad (25)$$

where we have used $(f_1 f_2)(x) = f_1(x) f_2(x)$. Using boundary conditions (23)₂ and (23)₃ in (25) and then simplifying leads to

$$\sigma = \frac{E_0 f^2(0) + E_1 f^2(-L)}{\mu_r k f^2(0) + \mu_l k f^2(-L) + \mu_1 \int_{-L}^0 (k^2 f^2 + f_x^2) dx}. \quad (26)$$

All the terms in the denominator above are positive.

In (26), if we neglect appropriate positive terms from the denominator and negative terms from the numerator if any; then we get the following four cases:

$$k^2 > \max \left\{ \frac{U[\mu]_l}{T_1}, \frac{U[\mu]_r}{T_0} \right\} \Rightarrow E_0 < 0, \quad E_1 < 0 \Rightarrow \sigma < 0, \quad (27)$$

$$\frac{U[\mu]_r}{T_0} < k^2 < \frac{U[\mu]_l}{T_1} \Rightarrow E_0 < 0, \quad E_1 > 0 \Rightarrow \sigma < \frac{E_1}{\mu_1 k}, \quad (28)$$

$$\frac{U[\mu]_l}{T_1} < k^2 < \frac{U[\mu]_r}{T_0} \Rightarrow E_0 > 0, \quad E_1 < 0 \Rightarrow \sigma < \frac{E_0}{\mu_r k}, \quad (29)$$

$$k^2 < \min \left\{ \frac{U[\mu]_l}{T_1}, \frac{U[\mu]_r}{T_0} \right\} \Rightarrow E_0 > 0, \quad E_1 > 0 \Rightarrow \sigma < \frac{E_0 f^2(0) + E_1 f^2(-L)}{\mu_r k f^2(0) + \mu_1 k f^2(-L)}, \quad (30)$$

for a non-trivial disturbance. We first consider the upper bound on the growth rates of waves in the range

$$k^2 < \min \left\{ \frac{U[\mu]_r}{T_0}, \frac{U[\mu]_l}{T_1} \right\}, \quad (31)$$

where the inequality (30) for the growth rate σ holds. To this inequality, we apply the following relation from [9] which holds for arbitrary n under the condition $A_i > 0, B_i > 0, X_i > 0$, for $i = 1, \dots, n$,

$$\frac{\sum_i^n (A_i X_i)}{\sum_i^n (B_i X_i)} \leq \max_i \left\{ \frac{A_i}{B_i} \right\}. \quad (32)$$

Then we obtain for waves in the range (31)

$$\sigma(k) < \max \left\{ \frac{E_0}{k\mu_r}, \frac{E_1}{k\mu_1} \right\} = \max \left\{ \left(\frac{[\mu]_r Uk - T_0 k^3}{\mu_r} \right), \left(\frac{[\mu]_l Uk - T_1 k^3}{\mu_1} \right) \right\}, \quad (33)$$

where we recall $[\mu]_r = (\mu_r - \mu_1)$, and $[\mu]_l = (\mu_1 - \mu_l)$. Since the upper bound (33) is not less than the estimates (28) and (29) for the upper bounds on growth rates for waves outside the range (31), (33) is a modal upper bound for all waves. The absolute upper bound (i.e., the growth rate of any unstable wave cannot exceed this bound) is then given by

$$\sigma < \max \left\{ \frac{2T_0}{\mu_r} \left(\frac{U[\mu]_r}{3T_0} \right)^{3/2}, \frac{2T_1}{\mu_1} \left(\frac{U[\mu]_l}{3T_1} \right)^{3/2} \right\}. \quad (34)$$

Below, in lemma 1 we obtain an estimate for the integral in the denominator of (26) which was neglected in the above estimate. This estimate will then be used to obtain a new upper bound for this three-layer case which, as we will see, is an improvement over (33) and (34).

3.2. A useful lemma

We need the following lemma to obtain the improved upper bound.

Lemma 1. Consider the function f and the integral I such that

$$f_{xx}(x) - k^2 f(x) = 0, \quad \forall x \in (-L, 0), \quad I = \int_{-L}^0 (k^2 f^2 + f_x^2) dx. \quad (35)$$

Then we have the inequality

$$I \geq k \tanh(kL) (\lambda_1 f^2(-L) + \lambda_2 f^2(0)), \quad (36)$$

where $\tanh(x) = (\exp(x) - \exp(-x))/(\exp(x) + \exp(-x))$, $\lambda_i \geq 0$, and $\lambda_1 + \lambda_2 \leq 1$.

Proof. The general solution of equation in (35) in terms of boundary data for the eigenfunction f is given by

$$f(x) = \frac{f(0) \sinh(kx + kL) - f(-L) \sinh(kx)}{\sinh(kL)}, \quad (37)$$

from which we have

$$\begin{aligned} f_x(0) &= \frac{k}{\sinh(kL)} \{f(0) \cosh(kL) - f(-L)\}, \\ f_x(-L) &= \frac{k}{\sinh(kL)} \{f(0) - f(-L) \cosh(kL)\}. \end{aligned} \quad (38)$$

We use (35), (38) and get

$$\begin{aligned} I &= \int_{-L}^0 (f_x f)_x dx = f(0) f_x(0) - f(-L) f_x(-L) \\ &= \frac{k}{\sinh(kL)} \{f(0)^2 \cosh(kL) - 2f(0) f(-L) + f^2(-L) \cosh(kL)\}. \end{aligned} \quad (39)$$

It is easy to see that the following inequality holds for the quadratic form F given below:

$$F(\zeta, \chi) = \frac{1}{\sinh b} \{\zeta^2 \cosh b - 2\zeta\chi + \chi^2 \cosh b\} \geq \tanh b \chi^2. \quad (40)$$

For this, a new form of the above inequality is considered which is useful for our purposes:

$$\zeta^2 \cosh b - 2\zeta\chi + \chi^2 \left\{ \cosh b - \frac{\sinh^2 b}{\cosh b} \right\} \geq 0. \quad (41)$$

We recall the formula $\cosh^2 b - \sinh^2 b = 1$. Then the last inequality is equivalent to

$$\zeta^2 \cosh b - 2\zeta\chi + \chi^2 \frac{1}{\cosh b} = \left(\zeta \sqrt{\cosh b} - \frac{\chi}{\sqrt{\cosh b}} \right)^2 \geq 0. \quad (42)$$

Since $F(\zeta, \chi)$ is symmetric in ζ and χ , the inequality (40) also holds if ζ and χ are interchanged in this equality. Then we have

$$F(\chi, \zeta) = \frac{1}{\sinh b} \{ \zeta^2 \cosh b - 2\zeta\chi + \chi^2 \cosh b \} \geq \tanh b \zeta^2. \quad (43)$$

Recall that $\cosh b \geq 1, \sinh b > 0, \forall b > 0$. Taking a convex combination of the two inequalities (40) and (43) and then using the resulting inequality in (39) with $\zeta = f(0), \chi = f(-L), b = kL$, we obtain the inequality (36) with $\lambda_1 + \lambda_2 = 1$. However, if the inequality (36) holds for $\lambda_1 + \lambda_2 = 1$, then it must also hold for $\lambda_1 + \lambda_2 \leq 1$ as each of the two additive terms in this inequality is positive. \square

Lemma 2. *The integral I defined in (35) satisfies the following inequality:*

$$I \geq \max \{ k \tanh(kL) f^2(-L), k \tanh(kL) f^2(0) \} \geq k \tanh(kL) (\lambda_1 f^2(-L) + \lambda_2 f^2(0)), \quad (44)$$

where $\lambda_i \geq 0$, and $\lambda_1 + \lambda_2 \leq 1$.

Proof. Regarding the best choice for the pair (λ_1, λ_2) in lemma 1 above so that we have the upper lower bound of integral I in (35), the following main result of linear programming theory (also known as the simplex method) is useful: ‘The maximum value of a linear function f on a convex set S is attained at one of the edges of S .’

Let $S = \{x, y | x, y, \geq 0, x + y \leq 1\}$ be the convex set between the lines $x = 0, y = 0, y = 1 - x$. Edges of S are the points $A = (0, 0), B = (1, 0)$, and $C = (0, 1)$. The linear function is $f(x, y) = ax + by, a, b > 0, x, y \geq 0$. The maximum value of f on S is attained either at A or at B or at C . But $f(A) = 0 < f(B)$ and $f(A) = 0 < f(C)$. Then the maximum value of f on S is attained in B or in C , which are the edges of the segment $x + y = 1$ intersecting with S . Then the conclusion is that the maximum value of f is attained either at $(1, 0)$ or at $(0, 1)$, Then the best possible choices of the two parameters are $(\lambda_1 = 1, \lambda_2 = 0)$ and $(\lambda_1 = 0, \lambda_2 = 1)$. This proves (44). \square

To obtain an improved absolute upper bound compared to (34), the inequality (44) needs to be used in (26) for the integral in the denominator which was earlier neglected to obtain (34). Because the inequality (44) depends on two parameters and the $\tanh(kL)$ term, a straightforward use of this will give a bound that depends on these, as we will see below. We have to seek values of the parameters and k which give the best absolute upper bound. To methodically do this, we introduce below different types of upper bounds and by analyzing these bounds, we obtain best absolute upper bound but only in terms of two constants which arise due to the $\tanh(kL)$ term. To get estimates of these constants, some analysis involving short and long waves is necessary for reasons discussed in section 3.6.

3.3. Some notation

For the rest of Part I (constant viscosity fluid layers) of the paper, the above two lemmas will be used to obtain several results on the upper bound on the growth rate in several kinds of flows. Because of there being two parameters (see inequalities (36) and (44)) in the above lemma, these parameters will appear often and we need a convention for notation for various upper bounds, some of which will depend on these parameters and

some of which will not. For ease of reference, whenever necessary while reading the rest of the paper, we give this notation here.

- $\lambda_{i,j}$: this notation is a generalization of the notation λ_1 and λ_2 used in the lemma above. This is required for multi-layer flows as we will see in later sections. The first subscript ‘ i ’ on $\lambda_{i,j}$ can be either 1 or 2 in the spirit of the lemma (see (36)). As we will see below, an inequality of the type (36) will appear for each internal layer for multi-layer flows. The second index ‘ j ’ on $\lambda_{i,j}$ refers to the specific internal-layer number ‘ j ’ in multi-layer flows. Below, we do not use this second index when there is only one internal layer, i.e., in the three-layer case, because there is no source of confusion in not using this second index in this case. In general, however, for flows with more than one internal layer we will use $\lambda_{i,j}$ in the notation when using the above lemma.
- $\sigma_n(k)$: this notation stands for the *exact* value of the growth rate $\sigma_n(k)$ of a mode with wavenumber k in $(n+2)$ -layer Hele-Shaw flows which has n internal layers ($n = 1, 2, N$ are of interest below).
- $\sigma_n^m(k; \lambda_{i,j})$: this notation stands for the *modal upper bound* on $\sigma_n(k)$ which depends on parameters $\lambda_{i,j}$. In other words, $\sigma_n(k) \leq \sigma_n^m(k; \lambda_{i,j})$ for all allowable values of $\lambda_{i,j}$ according to lemma 1. The exact number of parameters that it will depend on will be exactly $2n$ and this will be explicit in the expression for $\sigma_n^m(k; \lambda_{i,j})$.
- $\sigma_n^m(k)$: this stands for the *modal upper bound independent of parameters* $\lambda_{i,j}$. Physically, this is of interest. Thus it is defined as

$$\max_{\lambda_{1,j} + \lambda_{2,j} \leq 1} \sigma_n^m(k; \lambda_{i,j}) \leq \sigma_n^m(k).$$

This maximum is to be taken over all layers, i.e., $\lambda_{1,j} + \lambda_{2,j} \leq 1$, $\forall 1 \leq j \leq n$.

- $\sigma_n^u(\lambda_{i,j})$: this is the *absolute upper bound* over all wavenumbers for any specific choice of parameters within the constraint of lemma 1.
- σ_n^u : this is the *absolute upper bound* over all wavenumbers and over all allowable values of the parameters $\lambda_{i,j}$. Growth rates cannot exceed this value regardless of the value of k and parameters $\lambda_{i,j}$. Thus

$$\max_k \sigma_n^m(k) \leq \sigma_n^u = \max_{\lambda_{i,j}} \sigma_n^u(\lambda_{i,j}).$$

Below, when necessary we will use either s or l subscript on σ in addition to n to denote short wave or long wave regimes respectively.

3.4. New improved results on the upper bound

Using inequality (36) of the above lemma in (26) and then using inequality (32) gives the following modal upper bound $\sigma_1^m(k; \lambda_1, \lambda_2)$ (subscript 1 on σ is now used here to indicate the case of one internal layer or equivalently three-layer flows) for any specific choice for the values of (λ_1, λ_2) within the constraint of lemma 1:

$$\begin{aligned} \sigma_1(k) &\leq \frac{([\mu]_r Uk - T_0 k^3) f^2(0) + ([\mu]_l Uk - T_1 k^3) f^2(-L)}{(\mu_r + \lambda_2 \mu_1 \tanh(kL)) f^2(0) + (\mu_l + \lambda_1 \mu_1 \tanh(kL)) f^2(-L)} \\ &\leq \max \left\{ \frac{[\mu]_l Uk - T_1 k^3}{\mu_l + \lambda_1 \mu_1 \tanh(kL)}, \frac{[\mu]_r Uk - T_0 k^3}{\mu_r + \lambda_2 \mu_1 \tanh(kL)} \right\} \end{aligned}$$

$$\begin{aligned}
&= \max \{Q_1(k, \lambda_1), Q_r(k, \lambda_2)\} \\
&= \sigma_1^m(k; \lambda_1, \lambda_2).
\end{aligned} \tag{45}$$

For purposes below, we have used above the notation

$$\begin{aligned}
Q_1(k, \lambda_1) &= ([\mu]_1 Uk - T_1 k^3) / (\mu_1 + \lambda_1 \mu_1 \tanh(kL)), \\
Q_r(k, \lambda_2) &= ([\mu]_r Uk - T_0 k^3) / (\mu_r + \lambda_2 \mu_1 \tanh(kL)).
\end{aligned} \tag{46}$$

Since the modal upper bound $\sigma_1^m(k; \lambda_1, \lambda_2)$ is in terms of two parameters λ_1 and λ_2 , we have two families of upper bounds in (45). We derive such formulae in sections 4 and 5 for four-layer (see (90)) and N -layer (see (99)) flows respectively. For the choice of $(\lambda_1, \lambda_2) = (0, 0)$, the modal upper bound $\sigma_1^m(k; \lambda_1, \lambda_2)$ given by (45) reduces to the already known upper bound result given by (33). Since $\tanh(kL)$ is an increasing function of kL , the new upper bound $\sigma_1^m(k; \lambda_1, \lambda_2)$ given by (45) is certainly an improvement over (33) for any choice of $(\lambda_1, \lambda_2) \neq (0, 0)$. The modal upper bound $\sigma_1^m(k; \lambda_1, \lambda_2)$ for $\lambda_1 = \lambda_2 = \frac{1}{2}$ is an interesting upper bound because of the equal effects that these parameters produce on $Q_1(k, \lambda_1)$ and $Q_r(k, \lambda_2)$ (see (46) and (45)).

3.5. Best estimates on modal and absolute upper bounds

For the best possible estimate of the upper bound within the limitation of lemma 1, we need to use values of (λ_1, λ_2) for which the estimate (45) is the least over all admissible values of λ_1 and λ_2 . Therefore, using lemma 2, it is clear from the expression (45) that the desired estimate $\sigma_1^m(k)$ of the modal upper bound over all allowable values of λ_1 and λ_2 is given by

$$\begin{aligned}
\sigma_1(k) &\leq \min(\sigma_1^m(k; 1, 0), \sigma_1^m(k; 0, 1)) \\
&= \min\left(\max\left\{Q_1(k, \lambda_1 = 1), \right. \right. \\
&\quad \left. \left. Q_r(k, \lambda_2 = 0)\right\}, \max\{Q_1(k, \lambda_1 = 0), Q_r(k, \lambda_2 = 1)\}\right) \\
&= \min\left(\max\left\{\frac{[\mu]_1 Uk - T_1 k^3}{\mu_1 + \mu_1 \tanh(kL)}, \frac{[\mu]_r Uk - T_0 k^3}{\mu_r}\right\}, \right. \\
&\quad \left. \max\left\{\frac{[\mu]_1 Uk - T_1 k^3}{\mu_1}, \frac{[\mu]_r Uk - T_0 k^3}{\mu_r + \mu_1 \tanh(kL)}\right\}\right) \\
&= \sigma_1^m(k).
\end{aligned} \tag{47}$$

The functions $Q_1(k, \lambda_1 = 0)$ and $Q_r(k, \lambda_2 = 0)$ take their maximum values $Q_{1,\max}(\lambda_1 = 0)$ and $Q_{r,\max}(\lambda_2 = 0)$ at $k = k_{c,1}$ and $k = k_{c,2}$ respectively which are given by

$$\begin{aligned}
k_{c,1} &= \sqrt{\frac{U[\mu]_1}{3T_1}}, \quad k_{c,2} = \sqrt{\frac{U[\mu]_r}{3T_0}}, \\
Q_{1,\max}(\lambda_1 = 0) &= \frac{2T_1}{\mu_1} \left(\frac{U[\mu]_1}{3T_1}\right)^{3/2}, \quad Q_{r,\max}(\lambda_2 = 0) = \frac{2T_0}{\mu_r} \left(\frac{U[\mu]_r}{3T_0}\right)^{3/2}.
\end{aligned} \tag{48}$$

The denominator of $Q_1(k, \lambda_1)$ is an increasing function of k for $\lambda_1 \neq 0$ and therefore its effect on the parabolic profile in k of the numerator is to reduce the maximum value $Q_{1,\max}(\lambda_1 = 0)$ given by (48) and it appears as one of the terms in old estimate (34) of

the absolute upper bound. And similarly for $Q_{r,\max}(\lambda_2 = 0)$. Therefore, it should be clear that the estimate σ_1^u of the absolute upper bound based on the maximum values of the terms in (47) is an improvement over the previous estimate (34).

The following improved estimate σ_1^u of the absolute upper bound follows from (47) and (48):

$$\begin{aligned} \sigma_1(k) &\leq \min \left(\max \left\{ Q_{1,\max}(\lambda_1 = 1), \frac{2T_0}{\mu_r} \left(\frac{U[\mu]_r}{3T_0} \right)^{3/2} \right\}, \right. \\ &\quad \left. \max \left\{ \frac{2T_1}{\mu_l} \left(\frac{U[\mu]_l}{3T_1} \right)^{3/2}, Q_{r,\max}(\lambda_2 = 1) \right\} \right) \\ &= \sigma_1^u, \end{aligned} \tag{49}$$

where

$$Q_{1,\max}(\lambda_1 = 1) = \max_k \left(\frac{[\mu]_l Uk - T_1 k^3}{\mu_l + \mu_l \tanh(kL)} \right) = \left(\frac{[\mu]_l Uk_1^* - T_1 (k_1^*)^3}{\mu_l + \mu_l \tanh(k_1^* L)} \right), \tag{50}$$

and k_1^* is the value of k that solves the following equation:

$$\frac{[\mu]_l Uk - T_1 k^3}{\mu_l + \mu_l \tanh(kL)} = \frac{([\mu]_l U - 3T_1 k^2) \cosh^2(kL)}{\mu_l L}. \tag{51}$$

Similarly, formulae analogous to (50) and (51) can be written down for $Q_{r,\max}(\lambda_2 = 1)$ and the corresponding value of k_2^* respectively. One has to take recourse to numerical computation to first find k_1^*, k_2^* from (51) etc, and then find the upper bound σ_1^u using the above formulae (49). Below, we derive an approximation σ_1^a (see (53) below) of the bound σ_1^u (see (49) above) that does not require numerical computation.

Since $\tanh(kL)$ is an increasing function of its argument, we can obtain from (46) that

$$\begin{aligned} Q_{1,\max}(\lambda_1) &= \max_k \left(\frac{[\mu]_l Uk - T_1 k^3}{\mu_l + \lambda_1 \mu_l \tanh(kL)} \right) \\ &\leq \max_k \left(\frac{[\mu]_l Uk - T_1 k^3}{\mu_l + \lambda_1 \mu_l c_1} \right) \\ &= \frac{2T_1}{\mu_l + \lambda_1 \mu_l c_1} \left(\frac{U[\mu]_l}{3T_1} \right)^{3/2}, \end{aligned} \tag{52}$$

where $0 < c_1 < \tanh(k_1^* L) \approx \tanh(k_{c,1} L)$ ($k_{c,1}$ has been defined in (48)). Since $k_1^* < k_{c,1}$ (see the explanation given earlier in the paragraph preceding (49)), it is safe to choose a value for $c_1 \leq \tanh(k_{c,1} L)$. Note that formulae similar to (52) exist for $Q_{r,\max}(\lambda_2)$ with a constant $c_2 \leq \tanh(k_{c,2} L)$. Using these facts in (50) and in an analogous formula for $Q_{r,\max}(\lambda_2 = 1)$, we obtain from (49) the following approximate upper bound σ_1^a given explicitly in terms of the parameters of the problem, unlike the bound σ_1^u given in (49):

$$\begin{aligned} \sigma_1(k) &\leq \min \left(\max \left\{ \frac{2T_1}{\mu_l + \mu_l c_1} \left(\frac{U[\mu]_l}{3T_1} \right)^{3/2}, \frac{2T_0}{\mu_r} \left(\frac{U[\mu]_r}{3T_0} \right)^{3/2} \right\}, \right. \\ &\quad \left. \max \left\{ \frac{2T_1}{\mu_l} \left(\frac{U[\mu]_l}{3T_1} \right)^{3/2}, \frac{2T_0}{\mu_r + \mu_l c_2} \left(\frac{U[\mu]_r}{3T_0} \right)^{3/2} \right\} \right) \\ &= \sigma_1^a \sim \sigma_1^u. \end{aligned} \tag{53}$$

Note that the selection procedure for values of c_1 and c_2 in this formula has been discussed above. It should be clear that the bound σ_1^u given in (49), though requiring numerical computation for evaluating its value, is the best absolute upper bound obtained so far on the growth rate. The approximate one σ_1^a given above in (53) may not be an improvement over σ_1^u . However, both of these estimates are significant improvements over the previously known result (34).

3.6. Stability enhancement

In two-layer flows, a reduction in the jump in viscosity $\mu_r - \mu_1$ (see equation (2)) at an unstable interface has a stabilizing effect whereas a reduction in the value of the surface tension has a destabilizing effect. Therefore, stabilizing an unstable interface in an otherwise two-layer flow (fluid with viscosity μ_1 pushing fluid with viscosity μ_r) by introducing a third fluid having viscosity μ_1 with $\mu_1 < \mu_1 < \mu_r$ (the notation has been discussed above) requires that interfacial surface tensions must have reasonable values so as not to offset any gain in stabilization due to reduction in viscosity jump at the leading interface in this three-layer set-up. It is of interest to be able to mathematically quantify this in terms of fluid viscosities and interfacial surface tensions for the three-layer flows. We will do this below in this section after discussing the roles of short and long waves in this stabilization process.

Since surface tension primarily affects short waves and not long waves, it is possible that middle-layer fluid with $\mu_1 < \mu_1 < \mu_r$ in the three-layer flow suppresses the instability of long waves regardless of the surface tension values at the two interfaces. We need to mathematically investigate this issue in this three-layer case for several reasons. If this is indeed the case (as we will see below), then it will allow us to obtain estimates for the constants c_1 and c_2 that appear in the formula (53).

3.6.1. Role of long waves. Below we use subscript l to refer to ‘long’ wave regime. For the modal upper bound $\sigma_{1,l}^m(k; \lambda_1, \lambda_2)$ for long waves ($kL \ll 1$), the inequality (45) is approximated as

$$\sigma_{1,l}(k) < \sigma_{1,l}^m(k; \lambda_1, \lambda_2) \approx \max \left\{ \frac{kU(\mu_1 - \mu_1)}{\mu_1 + \lambda_1 k L \mu_1}, \frac{kU(\mu_r - \mu_1)}{\mu_r + \lambda_2 k L \mu_1} \right\}. \quad (54)$$

This approximate upper bound $\sigma_{1,l}^m(k; \lambda_1, \lambda_2)$ for long waves will be less than the Saffman–Taylor growth rate for long waves (see formulae (1)) if both of the following inequalities hold:

$$\frac{kU(\mu_1 - \mu_1)}{\mu_1 + \lambda_1 k L \mu_1} < \frac{kU(\mu_r - \mu_1)}{\mu_r + \mu_1}, \quad (55)$$

and

$$\frac{kU(\mu_r - \mu_1)}{\mu_r + \lambda_2 k L \mu_1} < \frac{kU(\mu_r - \mu_1)}{\mu_r + \mu_1}. \quad (56)$$

The inequality (55) leads to

$$\mu_r - \mu_1 < \frac{\mu_r - \mu_1}{\mu_r + \mu_1} (\mu_1 + \lambda_1 k L \mu_1) < \frac{\mu_r - \mu_1}{\mu_r + \mu_1} (\mu_1 + L \mu_1). \quad (57)$$

Since $\mu_1 + L\mu_1 < \mu_r + L\mu_r = \mu_r(1 + L)$, the above inequality becomes

$$\mu_1 < \mu_1 + \frac{\mu_r - \mu_1}{\mu_r + \mu_1} \mu_r(1 + L). \quad (58)$$

Similarly, inequality (56) leads to

$$\mu_r - \mu_1 < \frac{\mu_r - \mu_1}{\mu_r + \mu_1} (\mu_r + \lambda_2 k L \mu_1) < \frac{\mu_r - \mu_1}{\mu_r + \mu_1} (\mu_r + L\mu_1). \quad (59)$$

Since $\mu_r + L\mu_1 < \mu_r + L\mu_r = \mu_r(1 + L)$, the above inequality becomes

$$\mu_r - \frac{(\mu_r - \mu_1)\mu_r(1 + L)}{\mu_r + \mu_1} < \mu_1. \quad (60)$$

From (58) and (60),

$$\mu_r - \frac{(\mu_r - \mu_1)\mu_r(1 + L)}{\mu_r + \mu_1} < \mu_1 < \mu_1 + \frac{(\mu_r - \mu_1)\mu_r(1 + L)}{\mu_r + \mu_1}. \quad (61)$$

This is consistent with the requirement $\mu_1 < \mu_1 < \mu_r$. From (61), we have

$$\mu_r - \frac{(\mu_r - \mu_1)\mu_r(1 + L)}{\mu_r + \mu_1} < \mu_1 + \frac{(\mu_r - \mu_1)\mu_r(1 + L)}{\mu_r + \mu_1}, \quad (62)$$

or equivalently

$$(\mu_r - \mu_1) < 2 \frac{(\mu_r - \mu_1)\mu_r(1 + L)}{\mu_r + \mu_1}, \quad (63)$$

which, after cancelation of $(\mu_r - \mu_1)$ from both sides, simplifies to

$$(L + 1) > \frac{\mu_r + \mu_1}{2\mu_r} \Rightarrow L > \frac{\mu_1 - \mu_r}{2\mu_r}. \quad (64)$$

This relation always holds since $L > 0$ and $\mu_1 < \mu_r$. Therefore, all long wave disturbances ($kL \ll 1$) are less unstable in this three-layer set-up than in the two-layer set-up regardless of the values of interfacial surface tensions. Therefore, only stabilities of short waves are affected by surface tension whereas the viscosity μ_1 of the middle-layer fluid (with μ_1 and μ_r fixed) affects the stability of all waves.

3.6.2. Role of short waves. For $kL \geq 1$ (short wave regime), inequality (45) is

$$\sigma_{1,s}(k) < \sigma_{1,s}^m(k; \lambda_1, \lambda_2) = \max_{\lambda_1 + \lambda_2 = 1} \left\{ \frac{kU[\mu]_l - k^3 T_1}{\mu_1 + \lambda_1 c_1 \mu_1}, \frac{kU[\mu]_r - k^3 T_0}{\mu_r + \lambda_2 c_2 \mu_1} \right\}. \quad (65)$$

The subscript s above refers to the short wave regime: $kL \geq 1$. Recall from the line after equation (52) that $c_1 \leq \tanh(k_1^* L)$ with k_1^* defined as a root of equation (51) and c_2 is defined similarly. It is clear that we can take $c_1 = c_2 = \tanh(1) = 0.7616$ in the above relation (65) as well as in (53). This value of c will only provide a conservative estimate of the absolute upper bound since the actual value of c will usually be higher (but less than 1) as $\tanh(kL)$ is an increasing function of its argument. The terms in these modal upper bounds are similar in form to the formula (1) for the exact growth rate in the two-layer case, only μ_1 in the denominator now has a multiplicative term involving μ_1 . Below, we write c for both c_1 and c_2 and as justified above, we can safely take $c = \tanh(1)$.

3.6.3. *Sufficient conditions for stability enhancement.* Improvement in stability for these three-layer flows over the two-layer case requires that $\sigma_1^u < \sigma_{st}$. We, instead, use

$$\sigma_1^a < \sigma_{st}, \quad (66)$$

where we recall that the approximate upper bound σ_1^a on the growth rate is given by (53) and σ_{st} by (2). This leads to two inequalities:

$$\frac{2T_1}{\mu_l + \lambda_1 c \mu_1} \left(\frac{U(\mu_l - \mu_1)}{3T_1} \right)^{3/2} < \frac{2T}{(\mu_r + \mu_l)} \left(\frac{U(\mu_r - \mu_l)}{3T} \right)^{3/2}, \quad (67)$$

and

$$\frac{2T_0}{\mu_r + \lambda_2 c \mu_1} \left(\frac{U(\mu_r - \mu_1)}{3T_0} \right)^{3/2} < \frac{2T}{(\mu_r + \mu_l)} \left(\frac{U(\mu_r - \mu_l)}{3T} \right)^{3/2}. \quad (68)$$

These two inequalities are written in terms of λ_1 and λ_2 so that they cover all four cases arising from the above requirement of enhancement of stability. The inequalities (67) and (68), after simple manipulation, lead to respectively

$$\mu_l < \mu_l + \left(\frac{T_1}{T} \right)^{1/3} (\mu_r - \mu_l) \left(\frac{\mu_{1l}}{\mu_l + \mu_r} \right)^{2/3}, \quad (69)$$

and

$$\mu_r - \left(\frac{T_0}{T} \right)^{1/3} (\mu_r - \mu_l) \left(\frac{\mu_{r1}}{\mu_l + \mu_r} \right)^{2/3} < \mu_l, \quad (70)$$

where

$$\mu_{1l} = (\mu_l + \lambda_1 \mu_1 c), \quad \text{and} \quad \mu_{r1} = (\mu_r + \lambda_2 \mu_1 c). \quad (71)$$

The inequalities (69) and (70) when put together give

$$\mu_r - \left(\frac{T_0}{T} \right)^{1/3} (\mu_r - \mu_l) \left(\frac{\mu_{r1}}{\mu_l + \mu_r} \right)^{2/3} < \mu_l < \mu_l + \left(\frac{T_1}{T} \right)^{1/3} (\mu_r - \mu_l) \left(\frac{\mu_{1l}}{\mu_l + \mu_r} \right)^{2/3}. \quad (72)$$

Now, the above inequality (72) arising from the requirement of stability enhancement gives a lower (upper) bound on μ_l in terms of μ_r (μ_l), not inconsistent with $\mu_l < \mu_l < \mu_r$. The leftmost and rightmost parts of this inequality, after simple manipulation, give

$$\left(\frac{T_0}{T} \right)^{1/3} \left(\frac{\mu_{r1}}{\mu_l + \mu_r} \right)^{2/3} + \left(\frac{T_1}{T} \right)^{1/3} \left(\frac{\mu_{1l}}{\mu_l + \mu_r} \right)^{2/3} > 1, \quad (73)$$

or equivalently

$$\alpha \left(\frac{T_0}{T} \right)^{1/3} + \beta \left(\frac{T_1}{T} \right)^{1/3} > \left(\frac{\mu_l + \mu_r}{\mu_r^*} \right)^{2/3}, \quad (74)$$

where

$$\alpha = \left(\frac{\mu_{r1}}{\mu_r^*} \right)^{2/3}, \quad \text{and} \quad \beta = \left(\frac{\mu_{1l}}{\mu_r^*} \right)^{2/3}, \quad (75)$$

with $\mu_r^* = \mu_r + \max(\lambda_1, \lambda_2)c\mu_1$. The form of the inequality (74) is amenable to generalization for multi-layer flows as we will see later. For purposes below, it is better to rewrite (74) equivalently as

$$\left(\frac{T_0}{T}\right)^{1/3} + \left(\frac{\mu_1 + \lambda_1\mu_1c}{\mu_r + \lambda_2\mu_1c}\right)^{2/3} \left(\frac{T_1}{T}\right)^{1/3} > \left(\frac{\mu_r + \mu_1}{\mu_r + \lambda_2\mu_1c}\right)^{2/3}. \quad (76)$$

The significance of (76) should not be underestimated as it allows, for the purpose of enhancement of stability, selection of middle-layer fluids purely based on its interfacial tension properties for the extreme-layer fluids. It is appropriate here to recall the importance of the constraint $\mu_1 < \mu_r$. Only when $\mu_1 < \mu_r$ can criterion (76) be used to identify a class of middle-layer fluids for the purpose of enhancement of stability of two-layer fluid flows. Next, we consider some specific sufficient conditions arising from (76) for specific choices of the parameters λ_1 and λ_2 .

For the choice $(\lambda_1, \lambda_2) = (0, 0)$ corresponding to the upper bound (34), inequality (76) reduces to the sufficient condition

$$\left(\frac{T_0}{T}\right)^{1/3} + \left(\frac{\mu_1}{\mu_r}\right)^{2/3} \left(\frac{T_1}{T}\right)^{1/3} > \left(1 + \frac{\mu_1}{\mu_r}\right)^{2/3}. \quad (77)$$

Note that this particular sufficient condition (77) does not depend on the viscosity of the middle-layer fluid but it does depend on the interfacial tensions which certainly depend on this middle-layer fluid since both interfaces separate this middle-layer fluid from extreme-layer fluids. Notice that if $T_0 = T_1 = T$, then (77) reduces to an inequality which is always satisfied since, in general, it can be easily shown that $(1 + x^p) \geq (1 + x)^p$, $p \in (0, 1)$, $x \in [0, 1]$. (The proof for this is simple: consider the function $F(x) = (1 + x^p) - (1 + x)^p$. Then $F'(x) = p[x^{p-1} - (1 + x)^{p-1}]$. Since $(1 + x) \geq 1$ for $0 \leq x \leq 1$ and $(p - 1) < 0$, we have $0 < (1 + x)^{p-1} \leq 1$ and $x^{p-1} \geq 1$. Therefore $F'(x) > 0$ and since $F(0) = 0$, we have $F(x) > 0 \forall x \in [0, 1]$.) Therefore, if the surface tensions at interfaces separating every pair of these three fluids are the same, then we can always expect an enhancement of stability: a fact expected from physical insight.

For any other choice of (λ_1, λ_2) , the sufficient condition (76) depends on the viscosity μ_1 of the middle-layer fluid directly. For example, the choice of $(\lambda_1, \lambda_2) = (1, 0)$ in (76) gives the inequality

$$\left(\frac{T_0}{T}\right)^{1/3} + \left(\frac{\mu_1 + \mu_1c}{\mu_r}\right)^{2/3} \left(\frac{T_1}{T}\right)^{1/3} > \left(\frac{\mu_r + \mu_1}{\mu_r}\right)^{2/3}. \quad (78)$$

On the other hand, $(\lambda_1, \lambda_2) = (0, 1)$ in (76) gives the inequality

$$\left(\frac{T_0}{T}\right)^{1/3} + \left(\frac{\mu_1}{\mu_r + \mu_1c}\right)^{2/3} \left(\frac{T_1}{T}\right)^{1/3} > \left(\frac{\mu_r + \mu_1}{\mu_r + \mu_1c}\right)^{2/3}. \quad (79)$$

4. Four-layer flows

In this four-layer case, fluid flows at a constant velocity U in the direction of increasing viscosity with four layers, each having different but constant viscosity with positive viscosity jump in the direction of flow at each of the three planar interfaces (see figure 2). In a reference frame moving in the same direction as the flow with speed U , a fluid of

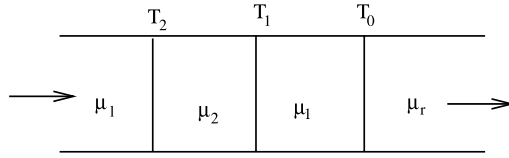


Figure 2. Four-layer fluid flow in a Hele-Shaw cell. The surface tensions at three interfaces are shown as $T_0, T_1,$ and T_2 . The constant viscosities are increasing in the direction of flow: $\mu_1 < \mu_2 < \mu_1 < \mu_r$.

viscosity μ_1 occupies an infinite region $x < -2L$ and a fluid of viscosity $\mu_r > \mu_1$ occupies an infinite region $x > 0$. Two intermediate regions $-L < x < 0$ and $-2L < x < -L$ have fluids of constant viscosities μ_1 and μ_2 respectively such that $\mu_1 < \mu_2 < \mu_1 < \mu_r$. It is clear that there are three interfaces located at $x = 0, -L,$ and $-2L$ with corresponding interfacial surface tensions denoted by $T_0, T_1,$ and T_2 respectively.

In this four-layer case, the relation (10) still holds away from all three interfaces and hence the relation (11) still holds in the exterior of the two internal layers of fluids with the obvious modification:

$$\begin{aligned} f(x) &= f(-2L) \exp(k(x + 2L)), & \text{for } x < -2L, \\ f(x) &= f(0) \exp(-kx), & \text{for } x > 0. \end{aligned} \tag{80}$$

Then we have $f_x^-(-2L) = kf(-2L)$ and $f_x^+(0) = -kf(0)$ in the exterior of the intermediate regions. The limit values of f_x on the boundaries of the two internal layers are given by formulae similar to (38). Using these limit values at the interfaces in the linearized dynamic and kinematic interfacial conditions, like in the three-layer case, after some algebraic manipulation, leads to the following three conditions at three interfaces, similar to (23):

$$\begin{aligned} -\mu_1(f_x^- f)(0) &= (\mu_r k - \sigma^{-1} E_0) f^2(0), \\ \mu_1(f_x^+ f)(-L) - \mu_2(f_x^- f)(-L) &= -\sigma^{-1} E_1 f^2(-L), \\ \mu_2(f_x^+ f)(-2L) &= (\mu_1 k - \sigma^{-1} E_2) f^2(-2L), \end{aligned} \tag{81}$$

where

$$\begin{aligned} E_0 &= k^2 U(\mu_r - \mu_1) - k^4 T_0, \\ E_1 &= k^2 U(\mu_1 - \mu_2) - k^4 T_1, \\ E_2 &= k^2 U(\mu_2 - \mu_1) - k^4 T_2. \end{aligned} \tag{82}$$

As before, we integrate equation (10) (which (9) reduces to in each layer) after multiplying with $f(x)$ on the interval $x \in (-2L, 0)$. In this interval, there is an interior interface at $x = -L$ across which there is a jump in the values of μ and $f_x(x)$. Therefore, we split the integral into two parts, namely on the intervals $(-2L, -L)$ and $(-L, 0)$. Thereby we get

$$-\mu_2 \int_{-2L}^{-L} (f_x f)_x dx - \mu_1 \int_{-L}^0 (f_x f)_x dx + \int_{-2L}^0 \mu f_x^2 dx + k^2 \int_{-2L}^0 \mu f^2 dx = 0. \tag{83}$$

Upon integration and simplifying, we get

$$\begin{aligned}
 & -\mu_2(f_x^- f)(-L) + \mu_2(f_x^+ f)(-2L) - \mu_1(f_x^- f)(0) \\
 & + \mu_1(f_x^+ f)(-L) + \int_{-2L}^0 \mu(f_x^2 + k^2 f^2) dx = 0.
 \end{aligned} \tag{84}$$

Using (81) in (84) and then simplifying, the growth rate can be expressed as

$$\begin{aligned}
 \sigma_2(k) &= \frac{E_0 f^2(0) + E_1 f^2(-L) + E_2 f^2(-2L)}{\mu_r k f^2(0) + \int_{-2L}^0 \mu(f_x^2 + k^2 f^2) dx + \mu_1 k f^2(-2L)} \\
 &= \frac{E_0 f^2(0) + E_1 f^2(-L) + E_2 f^2(-2L)}{\mu_r k f^2(0) + \mu_1 I_1 + \mu_2 I_2 + \mu_1 k f^2(-2L)},
 \end{aligned} \tag{85}$$

where

$$I_1 = \int_{-L}^0 (f_x^2 + k^2 f^2) dx, \quad \text{and} \quad I_2 = \int_{-2L}^{-L} (f_x^2 + k^2 f^2) dx.$$

The subscript 2 on σ above refers to the four-layer case. We use lemma 1 for these two integrals I_1 and I_2 in the above inequality. For each of these two integrals in lemma 1, we use different pairs of constants (see lemma 1). Our convention below will be to use a pair of constants $\lambda_{1,j}$ and $\lambda_{2,j}$ for internal layer j defined as the layer in $-jL < x < -(j-1)L$. Thus for integral I_1 which is over layer 1 (the rightmost internal layer), we use $\lambda_{1,1}$ and $\lambda_{2,1}$ in place of λ_1 and λ_2 respectively in lemma 1 (also see section 3.3). And similarly for other layers. Applying the lemma in this way, we obtain

$$\begin{aligned}
 \mu_1 I_1 + \mu_2 I_2 &\geq \mu_1 \{ \lambda_{1,1} f^2(-L) + \lambda_{2,1} f^2(0) \} k \tanh(kL) \\
 &+ \mu_2 \{ \lambda_{1,2} f^2(-2L) + \lambda_{2,2} f^2(-L) \} k \tanh(kL).
 \end{aligned} \tag{86}$$

The above two inequalities give us

$$\sigma_2(k) \leq \frac{E_0 f^2(0) + E_1 f^2(-L) + E_2 f^2(-2L)}{F_0 f^2(0) + F_1 f^2(-L) + F_2 f^2(-2L)}, \tag{87}$$

where the E_i are defined in (82) and the F_i are defined as follows:

$$\begin{aligned}
 F_0 &= k \{ \mu_1 \lambda_{2,1} \tanh(kL) + \mu_r \}, \\
 F_1 &= k (\mu_1 \lambda_{1,1} + \mu_2 \lambda_{2,2}) \tanh(kL), \\
 F_2 &= k \{ \mu_1 + \mu_2 \lambda_{1,2} \tanh(kL) \}.
 \end{aligned} \tag{88}$$

We are interested in the modal upper bounds on the growth rates of all waves. For reasons mentioned earlier in section 3.1, it is sufficient to analyze (87) for the upper bound when all $E_i > 0, i = 0, 1, 2$, in (87), i.e., when wavenumber k is in the range

$$k^2 \leq \min \left\{ \frac{U(\mu_2 - \mu_1)}{T_2}, \frac{U(\mu_1 - \mu_2)}{T_1}, \frac{U(\mu_r - \mu_1)}{T_0} \right\}. \tag{89}$$

Therefore we apply inequality (32) (for k in the range given by (89)) to (87) and obtain the following estimate of the upper bound on the growth rates of all waves:

$$\begin{aligned}\sigma_2(k) &\leq \max \left\{ \frac{E_0}{F_0}, \frac{E_1}{F_1}, \frac{E_2}{F_2} \right\} \\ &= \max_{\lambda_{1,j} + \lambda_{2,j} = 1} \left\{ \frac{(\mu_2 - \mu_1) Uk - T_2 k^3}{\mu_1 + \lambda_{1,2} \mu_2 \tanh(kL)}, \frac{(\mu_1 - \mu_2) Uk - T_1 k^3}{(\mu_1 \lambda_{1,1} + \mu_2 \lambda_{2,2}) \tanh(kL)}, \right. \\ &\quad \left. \frac{(\mu_r - \mu_1) Uk - T_0 k^3}{\mu_r + \lambda_{2,1} \mu_1 \tanh(kL)} \right\} \\ &= \sigma_2^m(k; \lambda_{1,1}, \lambda_{2,1}, \lambda_{1,2}, \lambda_{2,2}) \equiv \sigma_2^m(k; \lambda_{i,j}).\end{aligned}\quad (90)$$

The procedure that we outlined in section 3 after (46) can be used to derive estimates analogous to (47) and (49). Since this is straightforward, we omit this here.

4.1. Upper bounds based on asymptotics

It is difficult to obtain an absolute upper bound from (90) over the entire spectrum of wavenumbers for arbitrary values of the λ parameters within the constraint of lemma 1. However, for short waves and long waves, the asymptotic approximations to modal upper bound (90) are useful for the purposes of stability enhancement as before.

For $kL \ll 1$, the upper bound (90) can be approximated as

$$\begin{aligned}\sigma_{2,l}(k) &\leq \max \left\{ \frac{kU(\mu_2 - \mu_1)}{\mu_1 + \lambda_{1,2} kL \mu_2}, \frac{U(\mu_1 - \mu_2)}{L(\lambda_{2,2} \mu_2 + \lambda_{1,1} \mu_1)}, \frac{kU(\mu_r - \mu_1)}{\mu_r + \lambda_{2,1} kL \mu_1} \right\} \\ &= \sigma_{2,l}^m(k; \lambda_{i,j}).\end{aligned}\quad (91)$$

The second term in the above expression does not depend on k . Therefore, the modal upper bound (91) is not arbitrarily small for long waves, i.e., when k tends to zero. Compare this with modal upper bounds $\sigma_{st}(k)$ (see (1)) for the two-layer case and $\sigma_{1,l}^m(k)$ (see (54)) for the three-layer case. This shows that the stability of long waves may not always be enhanced in going from two- or three-layer flows to the four-layer flows considered here.

For short waves $kL \geq 1$, we have from (90)

$$\begin{aligned}\sigma_{2,s}(k) &\leq \max \left\{ \frac{(\mu_2 - \mu_1) Uk - T_2 k^3}{\mu_{2l}}, \frac{(\mu_1 - \mu_2) Uk - T_1 k^3}{\mu_{12}}, \frac{(\mu_r - \mu_1) Uk - T_0 k^3}{\mu_{r1}} \right\} \\ &= \sigma_{2,s}^m(k; \lambda_{i,j}),\end{aligned}\quad (92)$$

where $c \leq \tanh(k^*L)$ and

$$\mu_{r1} = (\mu_r + \lambda_{2,1} \mu_1 c), \quad \mu_{12} = (\lambda_{1,1} \mu_1 + \lambda_{2,2} \mu_2) c, \quad \mu_{2l} = (\mu_1 + \lambda_{1,2} \mu_2 c). \quad (93)$$

The subscript s in (92) refers to the ‘short’ wave regime as before. The terms in these modal upper bounds are similar in form to the formula (1) for the exact growth rate in the two-layer case. An absolute upper bound (i.e., independent of k but dependent on the parameters $\lambda_{i,j}$), denoted by $\sigma_{2,s}^u(\lambda_{i,j})$ and defined by $\sigma_{2,s}^u(\lambda_{i,j}) = \max_k \{\sigma_{2,s}^m(k; \lambda_{i,j})\}$ for

waves in this short wave regime, is then given by

$$\sigma_{2,s}(k) \leq \max \left\{ \frac{2T_0}{\mu_{r1}} \left(\frac{U[\mu]_0}{3T_0} \right)^{3/2}, \frac{2T_1}{\mu_{12}} \left(\frac{U[\mu]_1}{3T_1} \right)^{3/2}, \frac{2T_2}{\mu_{2l}} \left(\frac{U[\mu]_2}{3T_2} \right)^{3/2} \right\} \\ = \sigma_{2,s}^u(\lambda_{i,j}), \quad (94)$$

where $\lambda_{i,j}$ can take values within the constraint of lemma 1.

4.2. Sufficient conditions for stability enhancement

Improvement in stability for such four-layer flows over the two-layer case requires that the upper bound on the growth rate given by (94) be less than σ_{st} (see (2)). Using a procedure described in section 3.6.3, we obtain the following formula analogous to (73) of section 3.6.3:

$$\sum_{i=0}^{i=2} \alpha_i \left(\frac{T_i}{T} \right)^{1/3} \left(\frac{\mu_{i,i+1}}{\mu_l + \mu_r} \right)^{2/3} > 1 + \frac{(\mu_2 - \mu_1)}{(\mu_r - \mu_1)}, \quad (95)$$

where $\mu_{0,1} = \mu_{r1}$ and $\mu_{2,3} = \mu_{2l}$ as defined above in (93). Above, $\alpha_0 = 1, \alpha_1 = 2, \alpha_2 = 1$.

5. Multi-layer flows

Consider N intermediate regions of equal length L in the interval $(-NL, 0)$ in the rectilinear Hele-Shaw cell of infinite length. Each of these regions contains constant viscosity fluids with fluid of viscosity μ_l occupying the leftmost infinite region $x < -NL$ and fluid of viscosity μ_r occupying the rightmost infinite region $x > 0$. In the region $(-pL, -pL + L)$, with $p = 1, 2, \dots, N$, the viscosity of the fluid is μ_p such that $\mu_l = \mu_{N+1} < \mu_N < \mu_{N-1} < \dots < \mu_p < \mu_{p+1} < \dots < \mu_1 < \mu_0 = \mu_r$. We have $(N + 1)$ number of interfaces located at $x_i = -iL$, $i = 0, 1, 2, \dots, N$, and labeled as the i th interface. For $i = 0, 1, \dots, N$, we denote the surface tension coefficient on the i th interface at $x = x_i$ as T_i . Similarly, we use $[\mu]_i = \mu_i - \mu_{i+1}$ for the viscosity jump at the i th interface, $i = 0, 1, \dots, N$. The flow, as before, in the cell is in the direction of increasing viscosity. Recall the previous section. A quite similar procedure and lemma 1 give the following estimate:

$$\sigma_N \leq \frac{\sum_{i=0}^N E_i f^2(x_i)}{\sum_{i=0}^N F_i f^2(x_i)}, \quad (96)$$

where $E_i = k^2 U[\mu]_i - k^4 T_i$, $i = 0, 1, \dots, N$, and the F_i are defined as follows:

$$F_0 = k(\mu_l \lambda_{2,1} \tanh(kL) + \mu_r), \\ F_i = k(\mu_i \lambda_{1,i} + \mu_{i+1} \lambda_{2,i+1}) \tanh(kL), \quad i = 1, \dots, (N - 1), \\ F_N = k(\mu_l + \mu_N \lambda_{1,N} \tanh(kL)), \quad (97)$$

with $\lambda_{1,i} \geq 0, \lambda_{2,i} \geq 0$ such that $\lambda_{1,i} + \lambda_{2,i} \leq 1, \forall i = 1, \dots, N$. For reasons mentioned earlier in section 3.1, it is sufficient to analyze (96) for the upper bound for all $E_i > 0, i = 0, \dots, N$, in (96), i.e., when wavenumber k is in the range given by

$$k^2 \leq \min_i \left\{ \frac{U(\mu_i - \mu_{i+1})}{T_i} \right\}, \quad i = 0, 1, \dots, N. \quad (98)$$

Applying the inequality (32) to the above formula (96) for waves in the range given by (98), we obtain the following estimate of the modal upper bounds on the growth rates of all waves:

$$\begin{aligned}\sigma_N(k) &\leq \max_{\lambda_{1,i}+\lambda_{2,i}=1} \left\{ \frac{E_0}{F_0}, \frac{E_1}{F_1}, \dots, \frac{E_i}{F_i}, \dots, \frac{E_{N-1}}{F_{N-1}}, \frac{E_N}{F_N} \right\} \\ &\leq \max_{\lambda_{1,i}+\lambda_{2,i}=1} \{Q_0, Q_1, \dots, Q_i, \dots, Q_{N-1}, Q_N\} \\ &= \sigma_N^m(k; \lambda_{i,j}),\end{aligned}\tag{99}$$

where

$$\begin{aligned}Q_0 &= \frac{E_0}{F_0} = \frac{kU[\mu]_0 - k^3 T_0}{(\mu_r + \lambda_{2,1}\mu_1 \tanh(kL))}, \\ Q_i &= \frac{E_i}{F_i} = \frac{kU[\mu]_i - k^3 T_i}{(\lambda_{1,i}\mu_i + \lambda_{2,i+1}\mu_{i+1}) \tanh(kL)}, \quad i = 1, \dots, (N-1), \\ Q_N &= \frac{E_N}{F_N} = \frac{kU[\mu]_N - k^3 T_N}{(\mu_l + \lambda_{1,N}\mu_N \tanh(kL))}.\end{aligned}\tag{100}$$

Following the procedure outlined in section 3 after (46), one can judiciously choose the parameters $\lambda_{i,j}$ for the best modal upper bound $\sigma_N^m(k)$, analogous to (47), and for the best absolute upper bound σ_N^u , analogous to (49). The absolute upper bound arising from (99) will depend on parameters $\lambda_{1,j}$ and $\lambda_{2,j}$, $j = 1, \dots, N$. In this parameter space, this estimate is better with $(\lambda_{1,j}, \lambda_{2,j}) \neq (0, 0)$ even for some $j \in [1, N]$ than with $\lambda_{1,j} = \lambda_{2,j} = 0$, $\forall j = 1, \dots, N$. The best estimate of this absolute upper bound σ_N^u can be derived from (99) by the procedure outlined for the four-layer case in the previous section. In fact, it is easy to see that a similar procedure will give an expression for σ_N^u similar in form to (94) except that there will be $N + 1$ terms in its expression instead of three (see (94)). Since all this is straightforward along the lines of three-layer case treated earlier, we omit any further details here.

5.1. Sufficient conditions for stability enhancement

Using a procedure similar to those used for other cases (see section 3.6.3), we obtain the following generalization of the sufficient condition (95) from the four-layer case to this $(N + 2)$ -layer case:

$$\sum_{i=0}^{i=N} \alpha_i \left(\frac{T_i}{T} \right)^{1/3} \left(\frac{\mu_{i,i+1}}{\mu_l + \mu_r} \right)^{2/3} > 1 + \frac{(\mu_N - \mu_1)}{(\mu_r - \mu_l)},\tag{101}$$

where $\alpha_0 = 1, \alpha_N = 1, \alpha_i = 2$, for $i = 2, \dots, (N - 1)$, and

$$\begin{aligned}\mu_{0,1} &\equiv \mu_{r1} = \mu_r + \lambda_{2,1}\mu_1 c, \\ \mu_{i,i+1} &= (\lambda_{1,i}\mu_i + \lambda_{2,i+1}\mu_{i+1})c, \quad i = 1, 2, \dots, (N - 1), \\ \mu_{N,N+1} &\equiv \mu_{Nl} = \mu_l + \lambda_{1,N}\mu_N c.\end{aligned}\tag{102}$$

5.2. Upper bounds based on asymptotics

For long waves (i.e. $kL \ll 1$), using (96), (97), (99), and $\tanh(kL) \sim kL$, we obtain the modal upper bound $\sigma_{N,l}^m(k; \lambda_{i,j})$ for the individual wave with wavenumber k :

$$\sigma_{N,l}(k) \leq \sigma_{N,l}^m(k; \lambda_{i,j}) = \max \{Q_0^l, \dots, Q_p^l, \dots, Q_N^l\}, \quad (103)$$

where

$$\begin{aligned} Q_N^l &= \frac{kU(\mu_N - \mu_1)}{\mu_1 + \mu_N \lambda_{1,N} kL}, & Q_0^l &= \frac{kU(\mu_r - \mu_1)}{\mu_r + \mu_1 \lambda_{2,1} kL}, \\ Q_p^l &= \frac{U(\mu_p - \mu_{p+1})}{(\mu_p \lambda_{1,p} + \mu_{p+1} \lambda_{2,p+1})L}, & p &= 1, \dots, (N-1). \end{aligned} \quad (104)$$

For short waves with $kL \geq 1$, using (96), (97), and (99), we obtain an upper bound $\sigma_{N,s}^u(\lambda_{i,j})$ on the growth rate of waves in this short wave range:

$$\sigma_{N,s}(k) \leq \sigma_{N,s}^u(\lambda_{i,j}) = \max \{Q_0^s, \dots, Q_p^s, \dots, Q_N^s\}, \quad (105)$$

where

$$\begin{aligned} Q_0^s &= \frac{2T_0}{\mu_r + \lambda_{2,1} c \mu_1} \left(\frac{U(\mu_r - \mu_1)}{3T_0} \right)^{3/2}, & Q_N^s &= \frac{2T_N}{\mu_1 + \lambda_{1,N} c \mu_N} \left(\frac{U(\mu_N - \mu_1)}{3T_N} \right)^{3/2}, \\ Q_p^s &= \frac{2T_p}{(\lambda_{1,p} \mu_p + \lambda_{2,p+1} \mu_{p+1})c} \left(\frac{U(\mu_p - \mu_{p+1})}{3T_p} \right)^{3/2}, & p &= 1, 2, \dots, (N-1). \end{aligned} \quad (106)$$

5.3. Determination of the number of layers from the prescribed arbitrary growth rate of instability

In this section, we want to show that one can estimate the number of internal layers (N) that will ensure that the growth rate does not exceed a prescribed value, however small, when the viscosity jumps across all layers are equal. In this case, $\mu_i - \mu_{i+1} = (\mu_r - \mu_1)/(N+1)$. Therefore all viscosity jumps are equal. Moreover, we choose $\lambda_{i,p} = 1/2, \forall i, p$, for our estimations below. We estimate the above for short and long waves separately.

First, we estimate for long waves. It then follows from (104), after using the fact that $ka/(b+kc) < a/c$ for positive k, a, b, c , that

$$Q_0^l < Q^*, \quad Q_N^l < Q^*, \quad Q_p^l < Q^*/2, \quad \text{where } Q^* = \frac{2U(\mu_r - \mu_1)}{(N+1)L\mu_1}, \quad (107)$$

and hence from (103),

$$\sigma_{N,l}(k) \leq Q^* = \frac{2U(\mu_r - \mu_1)}{(N+1)L\mu_1}.$$

From this, we see that the number of layers can be determined *a priori* from the desired growth rate for long waves which can be as small as we please. For the growth rate not to exceed ε , this gives

$$(N+1) > \frac{2U(\mu_r - \mu_1)}{\varepsilon L \mu_1}. \quad (108)$$

Now for short waves, we use the estimate (106). Using the conditions $\mu_i > \mu_1$, $(\lambda_{1,i} + \lambda_{2,i})c \leq 1$, $\forall i = 1, \dots, N$, in (106), we obtain from (105)

$$\sigma_{N,s} \leq \frac{2T_{\min}}{\mu_1 c} \left(\frac{U(\mu_r - \mu_1)}{3(N+1)T_{\min}} \right)^{3/2}. \quad (109)$$

Therefore, to obtain a growth rate less than ε , however small, we get the following estimate for the number of layers of fluid:

$$(N+1) \geq \left(\frac{2}{\varepsilon \mu_1 c \sqrt{T_{\min}}} \right)^{2/3} \left(\frac{U(\mu_r - \mu_1)}{3} \right), \quad (110)$$

where $T_{\min} = \min\{T_0, T-1, \dots, T_N\}$. Finally, using the above results (108) and (110), we get

$$(N+1) > \max \left\{ \frac{2U(\mu_r - \mu_1)}{\varepsilon L \mu_1}, \frac{4^{1/3} U(\mu_r - \mu_1)}{3(\varepsilon \mu_1 c)^{2/3} (T_{\min})^{1/3}} \right\}, \quad (111)$$

which gives the number of layers required for $\sigma \leq \varepsilon$. Therefore, we can obtain a maximal growth rate as small as we please by increasing the number N of internal layers. Therefore, the two-layer Saffman–Taylor interfacial instability σ_{st} can be reduced by any factor desired simply by increasing the number of layers according to the relation (111). The number of layers according to (111) is likely to be so high (due to the small value of ε) that sufficient condition (101) will be automatically satisfied.

Part II: Variable viscosity fluid layers

We consider three- and four-layer flows below each layer having a smooth viscous profile with $\mu_x > 0$ in each layer. Below, we first review three-layer flows from [9] very briefly to recall the procedure in this variable viscosity case and to highlight the significance of the result. The procedure outlined will then be helpful in explaining the mathematical difficulty in obtaining similar results for the case of more than three layers in general. Moreover, the procedure provides a way for us to obtain some interesting results for the four-layer case as we will shortly see.

6. Three-layer flows

The three-layer case (see figure 3) is briefly reviewed here from [9] for reasons cited above. Multiplying (9) by $f(x)$ and then integrating on the interval $(-L, 0)$, we obtain

$$(\mu^+ f_x^+ f)(-L) - (\mu^- f_x^- f)(0) + \int_{-L}^0 \mu(f_x^2 + k^2 f^2) dx = \sigma^{-1} k^2 U \int_{-L}^0 \mu_x f^2 dx. \quad (112)$$

We recall the notation $(f_1 f_2)(x) = f_1(x) f_2(x)$ used before. Using boundary condition (21) in (112) and then simplifying leads to

$$\sigma = \frac{E_1 f^2(-L) + E_0 f^2(0) + k^2 U \int_{-L}^0 \mu_x f^2 dx}{\mu_l k f^2(-L) + \mu_r k f^2(0) + \int_{-L}^0 \mu(f_x^2 + k^2 f^2) dx}. \quad (113)$$

Note that all terms in the denominator of (113) are positive. As in earlier sections, it is sufficient to analyze (113) for the upper bound when $E_i > 0$, $i = 0, 1$, i.e., when

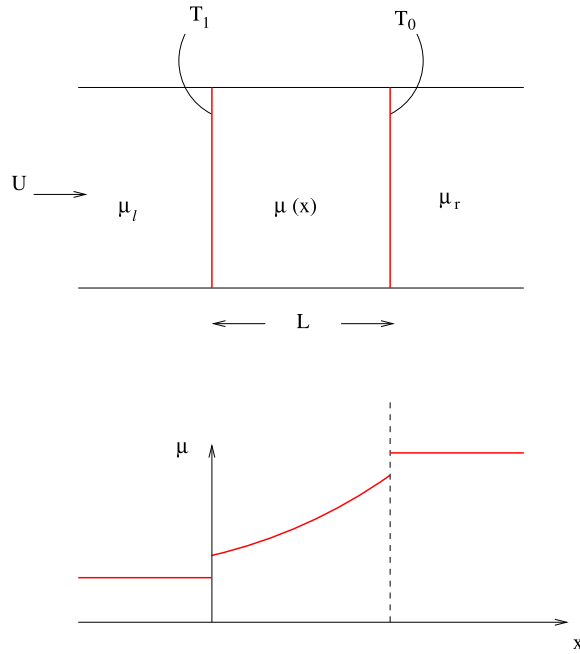


Figure 3. Three-layer fluid flow in a Hele-Shaw cell. The surface tensions at two interfaces are shown as T_0 and T_1 . The middle layer has variable viscosity. The flow is potentially unstable.

wavenumber k is in the range

$$k^2 < \min \left\{ \frac{U[\mu]_r}{T_0}, \frac{U[\mu]_l}{T_1} \right\}, \tag{114}$$

where $[\mu]_r = (\mu_r - \mu^-(0))$, and $[\mu]_l = (\mu^+(-L) - \mu_l)$. As before, applying the inequalities (32)–(113) for k in the range given by (114) (so that E_1 and E_2 are positive), we obtain after neglecting the positive term $\int_{-L}^0 \mu f_x^2$ in the denominator of (113) the following estimate of the upper bound on the growth rates of all non-trivial waves:

$$\begin{aligned} \sigma &< \max \left\{ \frac{E_1}{k\mu_l}, \frac{E_0}{k\mu_r}, \frac{U}{\mu_l} \sup_x \{\mu_x\} \right\} \\ &= \max \left\{ \frac{[\mu]_r U k - T_0 k^3}{\mu_r}, \frac{[\mu]_l U k - T_1 k^3}{\mu_l}, \frac{U}{\mu_l} \sup_x \{\mu_x\} \right\}. \end{aligned} \tag{115}$$

The absolute upper bound (i.e., the growth rate of any unstable wave cannot exceed this bound) is then given by

$$\sigma < \max \left\{ \frac{2T_0}{\mu_r} \left(\frac{U[\mu]_r}{3T_0} \right)^{3/2}, \frac{2T_1}{\mu_l} \left(\frac{U[\mu]_l}{3T_1} \right)^{3/2}, \frac{U}{\mu_l} \sup_x \{\mu_x\} \right\}. \tag{116}$$

For the ‘optimal’ viscosity profile given by

$$\sup_x (\mu_x) \leq \frac{\mu_l}{U} \max \left\{ \frac{2T_0}{\mu_r} \left(\frac{U[\mu]_r}{3T_0} \right)^{3/2}, \frac{2T_1}{\mu_l} \left(\frac{U[\mu]_l}{3T_1} \right)^{3/2} \right\}, \tag{117}$$

the estimate (115) becomes

$$\sigma < \max \left\{ \frac{2T_0}{\mu_r} \left(\frac{U[\mu]_r}{3T_0} \right)^{3/2}, \frac{2T_1}{\mu_l} \left(\frac{U[\mu]_l}{3T_1} \right)^{3/2} \right\}. \quad (118)$$

Note the significance of this result: if the limit viscosities $\mu^+(-L)$ and $\mu^-(0)$ at the two interfaces are close enough to μ_l and μ_r respectively and if we use the optimal profile (117) for the middle layer, then the upper bound on the growth rate becomes arbitrarily small and the flow is almost stable. However, to generate the optimal profile on the basis of this upper bound, length L of the middle layer can, in principle, be very large since the gradient of the viscosity at any point in the interior layer cannot exceed a predetermined small value which is dependent on the growth rate itself and (μ_l/U) according to relation (117).

We see from (113) that $\mu_x > 0$ for the middle layer has a destabilizing effect and $\mu_x < 0$ has a stabilizing effect. This also holds in the two-layer case with the middle-layer profile extending all the way up to $-\infty$ because in this case the first terms from the numerator and the denominator of (113) drop out. Such viscous profiles are automatically created when a shear thinning or shear thickening fluid is used as a displacing fluid. Therefore, if we just use this non-Newtonian property of these complex fluids within the Newtonian framework of this paper, then we expect similar kinds of stabilizations and destabilizations of instabilities when such fluids are used as displacing fluids. In fact, recent works on viscous fingering in complex fluids [16]–[21] show this to be the case even in the highly non-linear regime of viscous fingering. Therefore, in the absence of understanding based on exact non-linear theory of non-Newtonian complex fluids, we believe that our results and approach presented in this paper may be useful in interpreting some of the experimental results on viscous fingering in complex fluids.

7. Four-layer flows

The physical set-up here is same as in the constant viscosity case addressed in section 4 except that each of the two internal fluid layers has a smooth viscous profile $\mu(x)$ with $\mu_x > 0$. This flow has three interfaces, one at $x = 0$ with surface tension T_0 , and another two at $x = -L, -2L$ with surface tensions T_1, T_2 respectively. We assume that each of the two extreme interfaces at $x = -2L$ and 0 has positive viscosity jump in the direction of flow. The middle interface at $x = -L$ can have a similar positive viscosity jump in the direction of flow but, as we will see below, some interesting results can be obtained when the viscosity jump at this middle interface in the direction of flow is negative.

The mathematical problem is still defined by equation (9) in each layer, though this equation simplifies to (10) in the exterior layers: $x < -2L, x > 0$. Because of this, far-field behavior defined by (80) still holds, because of which $f_x^-(-2L) = kf(-2L)$ and $f_x^+(0) = -kf(0)$ on the exterior side of the outer two interfaces. The limit values of f_x on the boundaries of the two internal layers are given by formulae similar to (38). Using these limit values at the interfaces in the linearized dynamic and kinematic interfacial conditions, like in the four-layer constant viscosity case of section 4, after some algebraic manipulation, leads to the following three interfacial boundary conditions at $x = -2L, x = -L, x = 0$,

similar to (81):

$$\begin{aligned} -(\mu^- f_x^- f)(0) &= \mu_r k f^2(0) - \sigma^{-1} E_0 f^2(0), \\ (\mu^+ f_x^+ f)(-L) - (\mu^- f_x^- f)(-L) &= -\sigma^{-1} E_1 f^2(-L), \\ (\mu^+ f_x^+ f)(-2L) &= \mu_1 k f^2(-2L) - \sigma^{-1} E_2 f^2(-2L), \end{aligned} \quad (119)$$

where

$$\begin{aligned} E_0 &= E_0(k) = k^2 U[\mu_r - \mu^-(0)] - k^4 T_0, \\ E_1 &= E_1(k) = k^2 U[\mu^+(-L) - \mu^-(-L)] - k^4 T_1, \\ E_2 &= E_2(k) = k^2 U[\mu^+(-2L) - \mu_1] - k^4 T_2. \end{aligned} \quad (120)$$

In contrast with the constant viscosity case in section 4 where equation (10) was integrated, now equation (9) is integrated on the interval $x \in (-2L, 0)$ after multiplying with f as in the previous section. In this interval, $\mu(x)f_x(x)$ is discontinuous at the interior interface location $x = -L$. Therefore the integral is split into two parts, namely on the intervals $(-2L, -L)$ and $(-L, 0)$. Thus we get

$$\begin{aligned} -(\mu^- f_x^- f)(-L) + (\mu^+ f_x^+ f)(-2L) - (\mu^- f_x^- f)(0) + (\mu^+ f_x^+ f)(-L) + \int_{-2L}^0 \mu f_x^2 dx \\ + k^2 \int_{-2L}^0 \mu f^2 dx = \sigma^{-1} k^2 U \int_{-2L}^0 \mu_x f^2 dx. \end{aligned} \quad (121)$$

Using relations (119) in (121) and then simplifying we obtain

$$\sigma = \frac{E_2 f^2(-2L) + E_1 f^2(-L) + E_0 f^2(0) + k^2 \int_{-2L}^0 \mu_x f^2 dx}{\mu_1 k f^2(-2L) + \mu_r k f^2(0) + \int_{-2L}^0 \mu (f_x^2 + k^2 f^2) dx}. \quad (122)$$

We see that the numerator of (122) contains $f^2(-L)$ which does not appear in the denominator. Because of this, for positive viscosity jump in the direction of basic flow at each of the three interfaces (when $E_0, E_1, E_2 > 0$ for waves in the range given earlier in (89)) (122) cannot be reduced to a form to which the inequality (32) can be applied as we have done in previous cases to obtain an estimate of the upper bound in terms of the parameters of the problem. We can do so only if we allow the viscosity jump $(\mu^+(-L) - \mu^-(-L))$ at the interior interface at $x = -L$ to be negative, instead of positive, in the direction of basic flow. Then $E_1 < 0$ for waves in the range (89) and the term involving $f^2(-L)$ in the numerator of (122) is negative. Therefore, separating E_1 from the numerator recasts (122) as the difference between the ‘first part’ and the ‘second part’ where the ‘first part’ is a ratio similar in form to (113) and the ‘second part’ is a positive quantity proportional to $(\mu^-(-L) - \mu^+(-L))$. A consequence of this observation is that an absolute upper bound similar to (116) is obtained by neglecting the ‘second part’, namely

$$\sigma < \max \left\{ \frac{2T_0}{\mu_r} \left(\frac{U[\mu]_r}{3T_0} \right)^{3/2}, \frac{2T_2}{\mu_1} \left(\frac{U[\mu]_l}{3T_2} \right)^{3/2}, \frac{U}{\mu_1} \sup_x \{ \mu_x | x \neq -L, -2L, 0 \} \right\}. \quad (123)$$

We see that this absolute upper bound for the optimal profile (117) will be arbitrarily small if positive viscosity jumps at the $x = -2L$ and 0 interfaces in the direction of

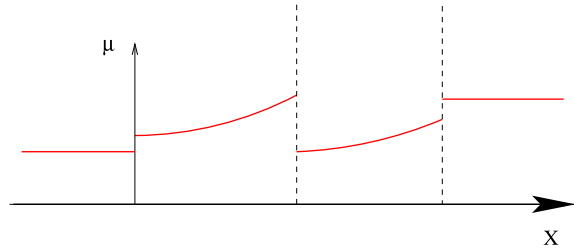


Figure 4. Four-layer fluid flow in a Hele-Shaw cell. The two internal layers have variable viscosity and thus each of these layers is potentially unstable individually. The two extreme interfaces are also unstable individually except for the internal interface. This multi-layer flow could be overall *potentially stable* if the internal interface is strongly stable on its own.

flow are small enough for reasons given after (117). Therefore, the maximum growth rate will be less than this absolute upper bound by a positive amount proportional to $\mu^-(-L) - \mu^+(-L) > 0$. If $(\mu^-(-L) - \mu^+(-L)) > 0$ is large enough, the maximum growth rate could be negative and the flow could be stable. Thus, in spite of the fact that internal layers and outer interfaces are individually unstable, this four-layer flow overall is stable only due to the middle interface being strongly stable on its own. Such a potentially stable configuration is shown in figure 4; keep in mind that the jumps in viscosities are not shown on a true scale.

Part III: Discussion and concluding remarks

8. Conclusions

In this paper, we have obtained the following results.

- (1) For three-layer Hele-Shaw flows with constant viscosity layers, a new absolute upper bound (53) on the growth rate of instabilities is obtained as a non-strict inequality. Thus, this bound can in principle be reached for a non-trivial disturbance. This is a considerable improvement over the absolute upper bound (34) which could not be reached for a non-trivial disturbance. A potential application of this is to control the instability of an interface separating low viscosity fluid from a high viscosity fluid that it is displacing. The way to do this is to introduce an intermediate layer of fluid with properties that will satisfy the two-parameter family of sufficient conditions (76) for enhancement of stability. The condition (77) is interesting because it does not depend on the viscosity $\mu \in (\mu_l, \mu_r)$ of the fluid in the middle layer. These results are of significance for the design of effective enhanced oil recovery methods.
- (2) We extended the above results to four-layer flows (see section 4), all layers having constant but different viscosity fluids. This four-layer case is important in setting the stage for a generalization to arbitrary number of layers of constant viscosity fluids and in exemplifying the difficulties associated with deriving similar results when internal layers have potentially unstable viscous profiles.
- (3) In section 5, the above mentioned results were generalized to arbitrary number of layers. As an application of these results, we have shown that the instability of

potentially unstable two-layer or three-layer flows with constant viscosity fluid layers can be significantly reduced to any desired level, however small, by increasing the number of layers (see section 5.3).

- (4) An absolute upper bound result for the three-layer case with potentially unstable middle layer is revisited. It is shown that extension of this to the four-layer case when both the internal layers and the three interfaces are individually unstable runs into difficulty with our approach. Thus this is an open problem. However, in this four-layer set-up, an absolute upper bound is obtained using our approach provided the middle interface is individually stable (meaning that the viscosity jump is negative in the direction of flow at this interface). In fact, we have shown that if this viscosity jump at the middle interface is large enough, the upper bound on the growth rate could in fact be negative and the flow overall could be stable.

Within the framework of the results itemized above, if one is to devise ways to significantly stabilize a viscosity jump driven unstable two-layer flow, there are three alternatives:

- (i) use of successive constant viscosity fluid layers with appropriate interfacial surface tensions so that sufficient conditions for stability enhancements are satisfied;
- (ii) use of a fluid layer in between whose viscous profile is optimal, given by (117), and where the limit viscosities $\mu^+(-L)$ and $\mu^-(0)$ at the two interfaces are close enough to μ_l and μ_r respectively;
- (iii) use of two internal fluid layers with viscous profiles of the internal layers such that the middle interface is strongly stable.

Towards this end, we must stress that many of the results obtained in this paper are general in character and that the techniques used hold promise for applications to other unstable multi-layer flows such as Rayleigh–Taylor unstable flows, coating flows, jet flows, and Kelvin–Helmholtz flow, to mention but a few. These results are obviously of fundamental and practical importance to many applications where stability of flows plays a decisive role. One instance of such an application is that of enhanced oil recovery by polymer flooding [5]–[7].

Acknowledgment

The author is grateful to two reviewers for their constructive criticisms which have helped us to improve the paper.

References

- [1] Hele-Shaw H S, *On the motion of a viscous fluid between two parallel plates*, 1898 *Trans R. Inst. Na. Archit. Lond.* **40** 218
- [2] Darcy H, 1856 *Les Fontaines Publiques de la Ville de Dijon* Victor Dalmond
- [3] Saffman P G and Taylor G I, *The penetration of a fluid in a porous medium or Hele-Shaw cell containing a more viscous fluid*, 1958 *Proc. R. Soc. A* **245** 312
- [4] Drazin P G and Reid W H, 1981 *Hydrodynamic Stability* (London: Cambridge University Press)
- [5] Slobod R L and Lestz J S, *Use of a graded viscosity zone to reduce fingering in miscible phase displacements*, 1960 *Producers Month.* **24** 12
- [6] Uzoigwe A C, Scanlon F C and Jewett R L, *Improvement in polymer flooding: the programmed slug and the polymer-conserving agent*, 1974 *J. Petrol. Tech.* **26** 33–41

- [7] Shah D and Schechter R, 1977 *Improved Oil Recovery by Surfactants and Polymer Flooding* (New York: Academic)
- [8] Daripa P and Pasa G, *On the growth rate for three-layer Hele-Shaw flows: variable and constant viscosity cases*, 2005 *Int. J. Eng. Sci.* **43** 877
- [9] Daripa P and Pasa G, *A simple derivation of an upper bound in the presence of viscosity gradient in three-layer Hele-Shaw flows*, 2006 *J. Stat. Mech.* P01014
- [10] Daripa P, *Studies on stability of three-layer Hele-Shaw flows*, 2008 *Phys. Fluids* **20** 112101
- [11] Daripa P and Pasa G, *New bounds for stabilizing Hele-Shaw flows*, 2004 *Appl. Math. Lett.* **18** 1293
- [12] Gorell S B and Homsy G M, *A theory of the optimal policy of oil recovery by the secondary displacement process*, 1983 *SIAM J. Appl. Math.* **43** 79
- [13] Saffman P G, *Viscous fingering in Hele-Shaw cells*, 1986 *J. Fluid Mech.* **173** 73
- [14] Howison S D, *Complex variable methods in Hele-Shaw moving boundary problems*, 1992 *Eur. J. Appl. Math.* **3** 209
- [15] Daripa P and Pasa G, *An optimal viscosity profile in enhanced oil recovery by polymer flooding*, 2005 *Int. J. Eng. Sci.* **42** 2029
- [16] Ben Amar M and Poire E C, *Pushing a non-Newtonian fluid in a Hele-Shaw cell: from fingers to needles*, 1999 *Phys. Fluids* **11** 1757
- [17] Chevalier C, Ben Amar M, Bonn D and Lindner A, *Inertial effects on Saffman–Taylor viscous fingering*, 2006 *J. Fluid Mech.* **552** 83
- [18] Lindner A, Bonn D, Poire E C, Ben Amar M and Meunier J, *Viscous fingering in non-Newtonian fluids*, 2002 *J. Fluid Mech.* **469** 237
- [19] Lindner A, Coussot P and Bonn D, *Viscous fingering in a yield stress fluid*, 2000 *Phys. Rev. Lett.* **85** 314
- [20] Lindner A, Bonn D and Meunier J, *Viscous fingering in a shear-thinning fluid*, 2000 *Phys. Fluids* **12** 256
- [21] Lindner A, Bonn D and Meunier J, *Viscous fingering in complex fluids*, 2000 *J. Phys.: Condens. Matter* **12** A477